Dear Editor,
Dear Delphine Farmer

We would like to thank the three reviewers, which with their valuable comments and suggestions helped to improve the manuscript.

Following the reviewer’s suggestions, we have carefully revised the manuscript. Please find below the point-by-point response to the reviewer comments. In addition, we attach a marked-up manuscript version highlighting all changes made.

With kind regards, on behalf of all co-authors,

Armin Hansel & Werner Jud

Anonymous Referee #1

Major comments

Overall, this is an excellent manuscript that relays exciting experimental results. The methodology is sound, and the authors have obvious expertise that is well conveyed. The quality of the manuscript is outstanding, and the majority of my minor comments are only for clarification of concepts. My only concern is the broader applicability of the results and the conclusions drawn about previous experiments in forested ecosystems. Viewing Fig 4, the effect is most strong for one variety of tobacco plant with particularly strong production of diterpeniods. How representative is the impact of the surface chemistry on the stomatal uptake of ozone? In particular, there is some language noted below under minor comments which should be more cautious in discussing results from the literature.

Author response: In the Atmospheric implications section of the revised manuscript we tried to make it clearer, why we think our results could be of importance in real world conditions. Just recently, Chan and co-workers reported a large variety of different semi-volatile, unsaturated diterpenoids found in a pine-forest (Chan et al., 2015), which seemed to be related to resins (known to contain high amounts of low-volatile di- and triterpenoids, see Langenheim, 2003) and followed a similar concentration time course as sequiterpenoids. Deposition of such semi-volatile compounds on leaves could have the same effect as the leaf exudates of our tobacco plants.
Unfortunately, to our knowledge until now there is only little data on the composition of substances deposited or exuded onto leaves (see Schmid et al., 1992; Bakker, 2000; Wagner et al., 2004; Himanen et al., 2010) and the broader applicability of our results does necessarily remain uncertain. We thus have followed the reviewer advice and altered our language reflecting this uncertainty. Most importantly, with regard to earlier works on non-stomatal ozone fluxes, we have clarified that these (ignoring the described surface reactions effect) should be considered as upper limits.

On a similar line, the fluid dynamics modeling adds an interesting dimension to the manuscript, but how applicable is it to the real world? For example, would surface heating due to light absorption affect the fluid dynamic results? Can this simulation produce realistic values for water vapour conductance?

Author response: The fluid dynamic simulations were included to "visualise the ozone concentration gradients caused by plant ozone uptake" and were thus, despite being based on first principles, not meant to simulate the real outdoor world where transport across the leaf boundary is governed by both forced and free convection and laminar/turbulent flow. Additionally, for water vapour different assumptions have to be made (non-zero concentration within the stomata), therefore these simulations are not directly applicable in the present form. However, the model simulations allow gaining a deeper understanding of the physical and chemical processes underlying the observed experimental results.
In the simulated flow regime the ozone transport in the leaf boundary layer is diffusion limited and convection caused by leaf heating plays only a minor role.

Minor comments

The use of conductance for interpreting the ozone loss in the chamber should be better integrated into the main text of the paper. For example, the concept is necessary for the discussion of Fig 3, but the concept is more fully introduced below. While the main explication of conductance can remain in the Appendix, there should be a brief description in the Methods section.

Author response: We added two new subsections (2.7 and 2.8) to the Methods part introducing the conductances and explaining why it is reasonable to use conductances instead of fluxes.

In addition, what is the area basis for the conductance measurement? Is it the one-sided leaf area? If so, are the exudates restricted to one side of the leaf? What is the area basis for the exudate experiments (Fig 3)?

Author response: The investigated diterpenoid exuding tobacco varieties have glandular trichomes on both the adaxial and the abaxial side. The area basis for the calculated conductances was, however, the one-sided leaf area. In the exudate experiments the area basis was the inner surface area of the enclosure system which was covered with leaf exudates. This information is now given in the new Methods subsection introducing the conductances (Sec. 2.8).

Page 19879, 21: "in H3O+ respectively NO+" should be "in H3O+ or NO+ respectively"

Author response: Done.

Page 19885, 11: Is there any GC/MS info about the content of the 3H02 leaf exudates?

Author response: We attach a chromatogram of *3H02* leaf exudates. The most prominent peaks in the chromatogram can be attributed to long chained alkanes, with octacosane being the largest one.

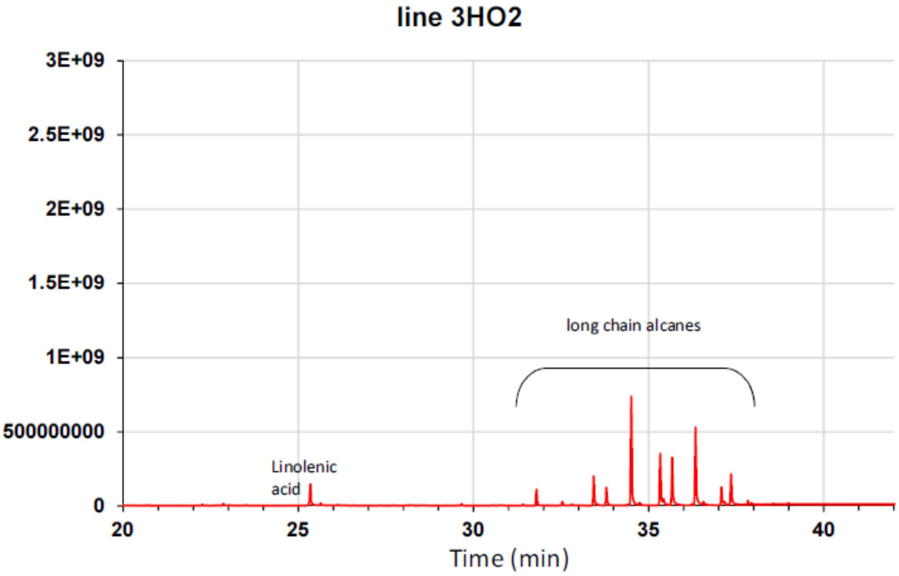

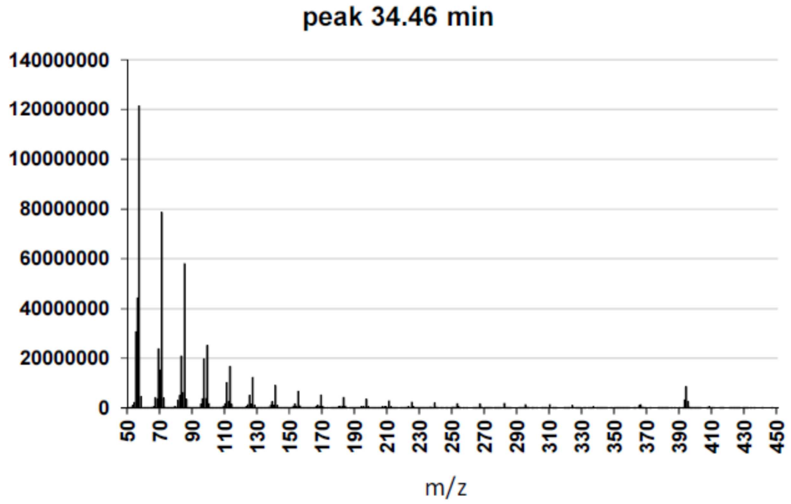

octacosane (C28 linear alcane)

Page 19886, 19: Make clear this is the microscopic simulation discussed in the Methods. Are the macroscopic results presented in the main text, or only the Supplement?

Author response: We changed the first sentence of this section to “Microscopic fluid dynamic model calculations revealed….”
The macroscopic results are presented in the supplement only. We added a sentence referencing to these in the fluid dynamic model calculations section.

Page 19887, 23: Provide an example reference.

Author response: We added an example reference (Monson & Baldocchi, 2014).

Page 19888, 17-18: Can any values for wind speed or u star be attached to this statement? Also, would small-scale convection due to leaf-surface heating have an effect?

Author response: We removed this statement.
In the simulated flow regime ozone transport in the leaf boundary layer is diffusion limited and convection caused by leaf heating plays only a minor role.

Page 19888, 20-25: But, this overestimation would depend strongly on the amount of unsaturated carbon-carbon double bonds located on the leaf surface. Referring to Figure 4 and variety 3H02, the effect could be relatively small. This is somewhat addressed in the final paragraph of Section 3.5 on the following page, but these statements should be qualified.

Author response: We rewrote this paragraph and clarified, that an overestimation of stomatal ozone uptake might be the case only if the surface of plants is covered with substantial amounts of unsaturated organic compounds and reported stomatal ozone uptake values in the cited studies should therefore be considered as upper limits.

Page 19889, 25-27: It’s great to put forward this hypothesis, but there is not enough justification to mention these initial results. Wait until the experiments are fully conducted, since no details are given in the current paper.

Author response: We removed the remark on our preliminary results.

Page 19890, 3-7: Should address observations in Karl et al 2010 (Science 5 November 2010: Vol. 330 no. 6005 pp. 816-819 DOI: 10.1126/science.1192534) which observed uptake of oxygenated VOCs in forest ecosystems.

Author response: We added a remark that the volatile carbonyl products from surface ozonolysis could to some part be taken up by the plants themselves and referenced Karl et al. (2010) and Niinemets et al. (2014).

Page 19890, 23-25: Could the experimental conditions have blocked the production of OH by the mechanism described by Liu et al 2014 (Science 26 September 2014: Vol. 345 no. 6204 pp. 1596-1598 DOI: 10.1126/science.1257158), since IR was excluded from the chamber?

Author response: We do not exclude the formation of OH radicals in the course of surface ozonolysis. In fact, gas-phase ozonolysis is the most important non-photolytic source of OH radicals in the Earth’s atmosphere. Criegee Intermediates are highly excited and are therefore very likely to decay, forming OH radicals, as we show in the Supplement. However, since OH is reacting fast with virtually all organic compounds, OH radicals produced at the surface will immediately be scavenged in surface assisted reactions with some organics (e.g. diterpenoids, waxes).

Fig. 1: What is the photograph in the background? This info should be given in the figure caption.

Author response: The background image shows glandular trichomes at the surface of a tobacco leaf. This information has been added to the figure caption.

Supplement Table S1: I understand having an atmospheric point of view to define uptake by plants as negative for an ecosystem, but the term assimilation only makes sense from the leaf point of view and uptake into the leaf should be positive.

Author response: Thank you for your suggestion. This data is now presented in Fig.4.

Anonymous Referee #2

The manuscript contribute to the state of the art, suggesting that previous research may have overestimated stomatal sink of ozone because surface reactions with O3 were not considered. This finding should be cautiously considered because only few plants emit very reactive VOC such as diterpenoids.

Author response: In the Atmospheric implications section of the revised manuscript we tried to make it clearer, why we think our results could be of importance in real world conditions. Just recently, Chan and co-workers reported a large variety of different semi-volatile, unsaturated diterpenoids found in a pine-forest (Chan et al., 2015), which seemed to be related to resins (known to contain high amounts of low-volatile di- and triterpenoids, see Langenheim, 2003) and followed a similar concentration time course as sequiterpenoids. Deposition of such semi-volatile compounds on leaves could have the same effect as the leaf exudates of our tobacco plants.
Unfortunately, to our knowledge until now there is only little data on the composition of substances deposited or exuded onto leaves (see Schmid et al., 1992; Bakker, 2000; Wagner et al., 2004; Himanen et al., 2010) and the broader applicability of our results does necessarily remain uncertain. We thus have followed the reviewer advice and altered our language reflecting this uncertainty. Most importantly, with regard to earlier works on non-stomatal ozone fluxes, we have clarified that these (ignoring the described surface reactions effect) should be considered as upper limits.

There are several methodological flaws which should be fixed in order to ameliorate the robustness of the research. The authors should clearly show the total O3 flux measured in the cuvette and compare the relative contribution of stomata vs surface deposition.

Author response: We included a new section (2.8) in the Methods part explaining why we use total ozone conductances instead of ozone fluxes to show differences between plants.
As we show in the Supplement, it is not possible to calculate stomatal and non-stomatal ozone fluxes exactly for plants with a semi-reactive leaf surface (which is likely the case for the tobacco varieties used in our experiments).

A graph showing total ozone fluxes and (estimated) stomatal ozone fluxes for each cultivar may help to better understand the results and convince the reader.

Author response: Please have a look at the new section (2.8) in the Methods part why we prefer do use total ozone conductances (presented in Fig. 4) rather than ozone fluxes when comparing different tobacco varieties. Exemplarily, we present the total ozone flux in Fig. 3 (former Fig. 2), showing results of an experiment using an *Ambalema* plant.

The role of stomata is not fully represented, since cultivars are compared but the stomatal conductance to water vapor is not clearly shown in the figures.

Author response: We added total water vapour conductance and assimilation rates to Fig. 4. We explain in the new methods part (section 2.8), why we were not able to calculate stomatal water vapour conductance.

I am convinced that the article pushes forward the state of the art with an initial effort to better investigate the role of reactive VOC in the O3 deposition. The paper should be published in ACP after replying these major comments:
Pag. 19874 lines 5-7: The striking questions assumes that poor research has been carried out to assess stomatal ozone uptake, but this is not true. The striking questions could be tuned in such a way: "Can surface reactions limit ozone entry through stomata and therefore reduce oxidative damage?"

Author response: We changed the striking question to "Can surface reactions limit the stomatal uptake of ozone and therefore reduce its detrimental effects to plants?"

Pag. 19877 lines 5-: There is information here which should go on setup section, i.e. the enclosed leaf surface. Line 10: why not to show also transpiration rate, or better stomatal conductance in the table? This help convincing the reader that stomata were closed at night. Photosynthesis alone is not sufficient to prove efficient stomatal closure at night.

Author response: We moved the sentence concerning the enclosed leaf area to the setup section. Total water vapour conductance values and assimilation rates are now presented in Fig. 4.

Pag. 19878 line 12: you mention that O3 concentration at the inlet was kept constant at 60 ppb. Did you measure O3 concentration outside the cuvette? It seems so, looking at the appendix. This may inform on the total O3 flux inside the cuvette and may be directly related to stomatal and non-stomatal processes. Figure 2 would benefit of O3 flux. In the appendix you show that O3 flux was measured, so why not to include it? As it is, the figure show that some diterpenoids are fast consumed by O3 supporting your thesis of relevant surface reactions, but the steady state of VOC suggests that surface reactions are important only in the first minutes and then what happens? Leaves stop removing O3? Or, perhaps, stomata keep sustaining O3 removal when surface reactions are negligible?

Author response: As mentioned in the setup section, ozone concentrations were measured at the inlet and at the outlet of the plant enclosure, switching in 2 min intervals between inlet and outlet. Inlet ozone concentrations were adjusted to obtain ~60-100 ppbv ozone at the cuvette outlet during light experiments. Please refer to Sec. 2.8 of the revised manuscript, why in general we use conductances and not ozone fluxes to compare different tobacco varieties or the same variety in light and dark conditions. As suggested, we exemplarily present the total ozone flux in Fig. 3 (former Fig. 2) now.
As we discuss in the main text and in the supplement, when starting ozone fumigation, diterpenoids deposited at *any* surface including leaves, the plant enclosure and the tubing system are reacting instantaneously with ozone. This can be seen in the large "burst" of volatile ozonolysis products when starting the ozone fumigation. The diterpenoids at the enclosure surface and enclosure outlet tubing were deposited during plant acclimatisation (while flushing the plant enclosure including the plant with ozone free air), which lasted typically 12-15 h. As the vapour pressure of the semi-volatile diterpenoids is rather small, it will take a long time to cover the tubing and the enclosure walls with

freshly exuded semi-volatile diterpenoids as these surfaces are most distant from the glandular trichomes. Starting the ozone fumigation, these surfaces are “cleaned” from diterpenoids by the fast ozone surface reactions. Consequently, as we mention in the figure caption, after a certain time, equilibrium between diterpenoid production and loss due to surface reactions (at the plant surface only) evolves, which results in stable signals of oxygenated VOC. We tried to make this clearer in Sec. 3.3 of the revised manuscript.

Pag. 19881 line 22: other papers after Laisk et al. show that O3 may accumulate in the stomata especially under high O3 concentration and low stomatal aperture, thus intercellular O3 concentration may be above 0. If the O3-reactive bottom of stomata is not perfect O3 scavenger, you may find that stomata are even less important, perhaps your model evaluation and discussion should consider this possibility.

Author response: Most of the current literature assumes intercellular O_3 concentrations to be close to zero, therefore we made the same assumption in our modelling approach (page 19888, line 13-14). Some recent papers use the work of Moldau and Bichele (2002) as reference for non-zero inter-cellular ozone concentrations. However, in their experiments, Moldau and Bichele (2002) used extremely high ozone concentrations (up to 1.14 ppmv), which are more than a factor of ten higher than we supplied. Anyway, non-zero intercellular ozone concentration would decrease the stomatal ozone uptake also in plants with non-reactive surface and is thus not specific for plants with ozone-reactive surface we discuss here. However, we now mention the possibility of non-zero intercellular ozone concentrations in the main text and discuss this in more detail in the Supplement. In Fig. S3 (which has now become Fig. S4) we replaced $c_i=0$ by c_i.

Pag. 19884 line23: Fig. S1 support your finding that surface reactions occurs fast to the plant surface, but the reactive surfaces are fast depleted of diterpenoids. The surface contribution to O3 removal is not continuous and this should be stressed in the text.

Author response: As we describe in the legend of figure S1 and in Sec.3 of the Supplement, the graph shows results from an experiment, in which two chambers (the first chamber containing a sample plant, the second chamber downstream containing no plant) were connected in series. During plant acclimatisation, some of the semi-volatile diterpenoids exuded by the sample plant were deposited on the surface of the second chamber and further downstream in the tubing. When we added ozone only to the second chamber, the diterpenoids deposited in the second chamber were consumed by ozone in about 1 h, after which the MVK signal, indicative for *cis*-abienol – ozone reactions, vanished. When we added ozone to the chamber containing the sample plant, initially the *cis*-abienol deposited onto the chamber wall was consumed and in part that on the plant surface. As mentioned above, after a certain time, an equilibrium between diterpenoid destruction by ozone and production by the plant trichomes was established, which eventually resulted in stable signals of oxygenated VOC. We have addressed this enclosure and plant tubing issue in several places in the manuscript (see e.g. page 19884, line 15; caption of Fig. 2) and the Supplement (Sec. 3). Fig. S2 shows that the surface reactions of ozone with *cis*-abienol in an experiment mimicking diurnal ozone variations resulted in a continuous production of MVK on two consecutive days, proving that the diterpenoids at the plant surface are not consumed fast.

Pag. 19885 line 19: Figure S3 shows that for several hours the O3 conductance in stripped leaves stays high (but still decreasing). You assess in the text that the ozone protection last for long periods (1,5 days as it seems in the figure S2). However the cis-abenol signal does not seem to fully recover after the dark period in Fig. S2, suggesting that manipulation of leaves may have produced unrealistic emissions of cis-abenol. Morover, spikes in MVK signals in Fig. S2 are not the same, suggesting that perhaps O3 concentration at the cuvette inlet were changed during the experiments? The dynamic of O3 at the cuvette outlet suggest that other factors influence the O3

flux in the cuvette. Please read my previous comments: the paper leave high uncertainty on the real O3 flux in the cuvette.

Author response: We assume the reviewer refers here to Fig. 3 (now Fig. 2) instead of Fig. S3, showing decreasing ozone conductances over several hours in experiments using leaf extracts. The O_3 conductance drops quickly for *3H02* leaf extract and lasts longer (several hours) for *Ambalema* leaf extracts. We discuss that the *Ambalema* extracts contain much more ozone reactive compounds (such as the diterpenoid *cis*-abienol) than the extracts of the *3H02* variety, which are consumed by surface ozonolysis reactions. In contrast to experiments using intact *Ambalema* plants, the *cis*-abienol is not refilled and consequently the O_3 conductance drops.
In the experiment with the *Ambalema* plant shown in Figure S2 the sample plant was kept in an almost ozone free surrounding for several weeks before the experiment started. This explains the slightly higher *cis*-abienol signal at the start of the experiment as compared to the *cis*-abienol signal after the 12 hours period of no ozone.
In course of the experiment we varied the inlet ozone concentration in order to mimic atmospheric diurnal ozone concentrations, explaining the varying outlet O_3 concentrations measured.
In this experiment during light conditions the total ozone flux consisted of stomatal and surface flux components. These are dependent on the ambient ozone concentrations (since $F_{O3}=g_{O3}*\Delta O_3$) and therefore, the relative contribution of the two flux components is changing with the ambient ozone concentration. This is the motivation why we use total ozone conductances instead of total ozone fluxes. While e.g. ozone flux to the cuticula is changing with the ambient ozone concentrations, we assume cuticular conductance to be constant under dark and light conditions and therefore changes in total ozone conductance when switching from dark to light conditions are mainly a result of increasing stomatal ozone conductance.

Pag 19885 line 27 and pag. 19886: Please see my previous comment: Fig.4 is convincing if you can demonstrate that stomata did not play a role at night for all tobacco varieties. You do this showing negligible rates of water transpiration at night for all varieties. Since you measured E (shown in the appendix), why not to discuss this?

Author response: Total water vapour conductance values and assimilation rates are now presented in Fig. 4. We discuss now in Sec. 3.4 why we think that stomatal conductance during dark phases cannot explain the observed effects on total ozone conductance.

Pag. 1988: the resistance scheme is clear, but the assumption that O3 is fully detoxified inside stomata may not be true.

Author response: See response above.

Anonymous Referee #3

General comments

This is an interesting manuscript with some innovative measurements and analyses concerning surface ozone reactions and their potential impact on atmospheric chemistry. I support publication but since there are some significant "mechanical" issues, the manuscript should undergo some major revision before publication since it could be much improved.

Specific comments

1. Intro: Ozone forecasts for future decades are indicated as being expected to increase (19875, line 15). However, as summarized recently by the IPCC (WG 1 report, 2013), tropospheric ozone is

expected to decline in the coming decades accept near densely populated regions. Meaning, only regionally higher ozone is expected.

Author response: We clarified that most parts of the Western hemisphere nowadays experience decreasing ozone background levels, while in Asia ozone background levels are still rising due to the increased emission of ozone precursor compounds (e.g. NO_x, methane).

2. The intro is too short overall. If I recall correctly, there are numerous previous works using tobacco plants to investigate ozone damage. I see few of those cited. A quick lit search on "ozone tobacco plant" reveals over 250 entries, some of which ought to be relevant. Also, the intro is worded as if contradicting previous works is the most important result of this work. I think not, especially since the authors have not demonstrated that the mechanism they investigated is an important one throughout the plant kingdom. See below.

Author response: We expanded the introduction by summarizing more literature on expected ozone trends and on the ozone tolerance of tobacco plants. We clarified that the described mechanism is only relevant for plants having very reactive leaf surfaces.

3. The measured ozone deposition values should be more clearly delineated from the conductance concept. The authors present results and analyses before they introduce the concept. Instead of an Appendix B, which is not referred to, the Methods section should be used (rather than section 3.5) to show how ozone flux was calculated, and adjusted (was it?). Ozone flux as plotted in the graphs is net ozone flux. Day-night differences distinguish surface-dominated losses versus total ozone losses. However, stomatal conductance and associated stomatal ozone losses are not presented although water vapor fluxes were calculated / used. For a proper comparison to previous work, stomatal conductances and photosynthesis rates need to be presented with the ozone fluxes. The current binary format of presentation in Figure 5 is useful but not quantitative. Wording such as "dramatic", and using percentages instead of multiples are symptomatic.

Author response: The conductance concept is now presented in the Methods part (Sec. 2.7). In the new section 2.8 we explain why we prefer to use total conductances instead of fluxes for the quantification of the ozone depletion capability of individual plants. Since with our setup it was not practical to calculate boundary layer conductances of water, stomatal conductance could not be calculated (see Sec. 2.8 of the revised manuscript). We implemented total water conductance and assimilation rates in Fig. 4.

4. The results sections should be rearranged to present the cis-abienol tests first, then the leaf surface extract tests, then the whole plant tests. This appears more logical to me. The current order is confusing and not goal-oriented.

Author response: We reordered the result section as suggested.

5. Atmospheric implications: The authors make swooping statements such as "plants will hardly lack any reactive surface compounds" and "Semi-volatile, unsaturated organic species are common on various surfaces including soil with plant litter, aerosols, sea surface layers, man-made structures and plant surfaces" without citing relevant studies. If this is supposedly common knowledge, at least give some examples.

Author response: We removed this statement and reformulated the atmospheric implications section, including more references.

As a result, we are made to believe that what was investigated can explain a wide variety of ozone deposition phenomena, but comparisons are missing. The Blodgett Forest studies are cited as one

such phenomenon, but the authors ignored that the suggested in-canopy gas-phase chemistry of ozone at that site was corroborated by measurements and a model that consider OH radical formation as result of the ozonolysis reactions. Thus surface reactions cannot be the dominant ozone loss mechanism at that site.

Author response: We reformulated this paragraph and tried to make clearer, why we think the described surface ozonolysis mechanism could be of importance in real outdoor environments.

I suggest that, to put the studied mechanism into perspective in terms of atmospheric implications, the authors look at measurements of nighttime ozone depletion at various sites with available data. They should consider ozone-NO and ozone-NO2 reactions, and, together with LAI data, compare ozone deposition rates to their laboratory data to judge whether the mechanism they investigated is likely to contribute widely to ozone losses from the troposphere (and in turn to SVOC emissions from the biosphere).

Author response: This is an excellent suggestion which we will follow up in another paper. The comparison with ecosystem-scale field measurements investigating different plant types would go beyond the scope of this paper.

6. The conclusion of a "powerful ozone protection mechanism" is thus neither quantitative nor justified. It also suggests that it is a purposeful mechanism instead of an opportunistic one. However, the latter is most likely correct since elevated ozone concentrations in the troposphere are highly unlikely to have existed before the advent of increasing fossil fuel combustion after the 2nd world war. Meaning, there was neither evolutionary pressure nor time to develop an "ozone protection mechanism". Respective wording in the manuscript should thus be altered.

Author response: Thank you for the suggestion, the wording has been changed to avoid misunderstanding of the intended meaning.

Lastly, since a qualitative or quantitative comparison to real-world situations is lacking, speculation that "some of the ozonolysis-derived products may play important roles in atmospheric processes, influencing the budgets of OH radicals and ozone" should be dropped as well, or at least qualified as speculative.

Author response: Done.

References:

Altimir, N., Vesala, T., Aalto, T., Bäck, J., and Hari, P.: Stomatal-scale modelling of the competition between ozone sinks at the air-leaf interface, Tellus, Series B: Chemical and Physical Meteorology, 60 B, 381–391, doi:10.1111/j.1600-0889.2008.00344.x, 2008.

Bakker M. I.: Atmospheric deposition of semivolatile organic compounds to plants, PhD Thesis, Ultrecht University, 2000

Chan, A. W. H., Kreisberg, N. M., Hohaus, T., Campuzano-Jost, P., Zhao, Y., Day, D. A., Kaser, L., Karl, T., Hansel, A., Teng, A. P., Ruehl, C. R., Sueper, D. T., Jayne, J. T., Worsnop, D. R., Jimenez, J. L., Hering, S. V., and Goldstein, A. H.: Speciated measurements of semivolatile and intermediate volatility organic compounds (S/IVOCs) in a pine forest during BEACHON-RoMBAS 2011, Atmos. Chem. Phys. Discuss., 15, 22331-22377, doi:10.5194/acpd-15-22331-2015, 2015.

Estell, R. E., Fredrickson, E. L., Anderson, D. M., Mueller, W. F., and Remmenga, M. D.: Relationship of

Tarbush Leaf Surface Secondary Chemistry to Livestock Herbivory, Journal of Range Management, 47, 424–428, doi:10.2307/4002991, 1994.

Estell, R. E., Havstad, K. M., Fredrickson, E. L., and Gardea-Torresdey, J. L.: Secondary chemistry of the leaf surface of Flourensia cernua, Biochemical Systematics and Ecology, 22, 73–77, doi:10.1016/0305-1978(94)90116-3, 1994.

Goldstein, A. H., McKay, M., Kurpius, M. R., Schade, G. W., Lee, A., Holzinger, R., and Rasmussen, R. A.: Forest thinning experiment confirms ozone deposition to forest canopy is dominated by reaction with biogenic VOCs, Geophys. Res. Lett., 31, L22106, doi:10.1029/2004GL021259, 2004.

Himanen, S. J., Blande, J. D., Klemola, T., Pulkkinen, J., Heijari, J., and Holopainen, J. K.: Birch (Betula spp.) leaves adsorb and re-release volatiles specific to neighbouring plants - a mechanism for associational herbivore resistance?, New Phytologist, 186, 722–732, doi:10.1111/j.1469-8137.2010.03220.x, 2010.

Karl, T., Harley, P., Emmons, L., Thornton, B., Guenther, A., Basu, C., Turnipseed, A. and Jardine, K.: Efficient atmospheric cleansing of oxidized organic trace gases by vegetation, Science, 330, 816–819, doi:10.1126/science.1192534, 2010.

Langenheim, J. H.: Plant Resins: Chemistry, Evolution, Ecology, and Ethnobotany, Timber Press, Portland, Cambridge, 2003.

Monson, R. and Baldocchi, D.: Terrestial Biosphere-Atmosphere Fluxes, Cambridge University Press, New York, 2014.

Niinemets, Ü., Fares, S., Harley, P., and Jardine, K. J: Bidirectional exchange of biogenic volatiles with vegetation: Emission sources, reactions, breakdown and deposition, Plant Cell Environ., 37, 1790–1809, doi:10.1111/pce.12322, 2014.

Schmid, C., Steinbrecher, R., and Ziegler, H.: Partition coefficients of plant cuticles for monoterpenes, Trees, 6, 32–36, doi:10.1007/BF00224496, 1992.

Wagner, G. J., Wang, E. and Shepherd, R. W.: New Approaches for Studying and Exploiting an Old Protuberance, the Plant Trichome, Annals of Botany, 93, 3–11, doi:10.1093/aob/mch011, 2004.

Marked-up version manuscript

Manuscript prepared for Atmos. Chem. Phys.
with version 2015/04/24 7.83 Copernicus papers of the LaTeX class copernicus.cls.
Date: 12 October 2015

Plant surface reactions: an ozone defence mechanism impacting atmospheric chemistry

W. Jud[1], L. Fischer[1], E. Canaval[1], G. Wohlfahrt[2,3], A. Tissier[4], and A. Hansel[1]

[1]Institute of Ion and Applied Physics, University of Innsbruck, 6020 Innsbruck, Austria
[2]Institute of Ecology, University of Innsbruck, 6020 Innsbruck, Austria
[3]European Academy of Bolzano, 39100 Bolzano, Italy
[4]Leibniz Institute of Plant Biochemistry, Department of Cell and Metabolic Biology,
06120 Halle, Germany

Correspondence to: A. Hansel (armin.hansel@uibk.ac.at)

Abstract. Elevated tropospheric ozone concentrations are considered a toxic threat to plants, responsible for global crop losses with associated economic costs of several billion dollars per year. Plant injuries have been linked to the uptake of ozone through stomatal pores and oxidative damage of the internal leaf tissue. But a striking question remains: how much ozone effectively enters the plant through open stomata and how much is lost by chemical reactions at the plant surfacecan surface reactions limit the stomatal uptake of ozone and therefore reduce its detrimental effects to plants?

In this laboratory study we could show that semi-volatile organic compounds exuded by the glandular trichomes of different *Nicotiana tabacum* varieties are an efficient ozone sink at the plant surface. In our experiments, different diterpenoid compounds were responsible for a strongly variety dependent ozone uptake of plants under dark conditions, when stomatal pores are almost closed. Surface reactions of ozone were accompanied by a prompt release of oxygenated volatile organic compounds, which could be linked to the corresponding precursor compounds: ozonolysis of *cis*-abienol ($C_{20}H_{34}O$) – a diterpenoid with two exocyclic double bonds – caused emissions of formaldehyde (HCHO) and methyl vinyl ketone (C_4H_6O). The ring-structured cembratrien-diols ($C_{20}H_{34}O_2$) with three endocyclic double bonds need at least two ozonolysis steps to form volatile carbonyls such as 4-oxopentanal ($C_5H_8O_2$), which we could observe in the gas phase, too.

Fluid dynamic calculations were used to model ozone distribution in the diffusion limited leaf boundary layer under daylight conditions. In the case of an ozone-reactive leaf surface, ozone gradients in the vicinity of stomatal pores are changed in such a way, that the ozone flux through the open stomata is strongly reduced.

Our results show that unsaturated semi-volatile compounds at the plant surface should be considered as a source of oxygenated volatile organic compounds, impacting gas phase chemistry, as well as efficient ozone sink improving the ozone tolerance of plants.

1 Introduction

Tropospheric ozone (O_3) is formed as a product of photochemical reactions involving nitrogen oxides (NO_x) and volatile organic compounds (VOC) as precursors (Jenkin and Clemitshaw, 2000). Increasing anthropogenic precursor emissions from fossil fuel and biomass burning have led to elevated ambient ozone concentrations over large portions of the earth's surface. Today, many regions experience near surface near-ground ozone background levels greater than 40 parts per billion volume (ppbv) (Vingarzan, 2004), levels which may be responsible for cellular damage inside leaves (Hewitt et al., 1990; Wohlgemuth et al., 2002) adversely affecting photosynthesis and plant growth (Ashmore, 2005). Toxic ozone concentrations cause visible leaf injury, plant damage and reduction in crop yields with associated economic costs of several billion dollars per annum worldwide (Wang and Mauzerall, 2004; Van Dingenen et al., 2009). Tropospheric ozone concentrations are expected to rise significantly through the next century especially during warm seasons, increasing the hazard of ozone damage to vegetation (Dentener et al., 2006; Sitch et al., 2007)Future trends of tropospheric ozone strongly depend on the emission factors of the corresponding precursor compounds (i.e. VOC and NO_x) and indirectly also on land cover and characteristics of the vegetation (Dentener et al., 2006; IPCC, 2013; Fu and Tai, 2015). Some recent studies revealed a stabilization or even a lowering of the tropospheric background ozone concentrations in parts of the industrialized western countries since the turn of the millennium (Logan et al., 2012; Parrish et al., 2012; Oltmans et al., 2013; IPCC, 2013). This is likely a result of preventive measures reducing ozone precursor emissions (Granier et al., 2011). In contrast, ozone background concentrations are still rising in parts of Asia experiencing high economic growth and a concomitant increase in NO_x emissions (Granier et al., 2011; Fu and Tai, 2015). Land cover and land use changes, often determined by changing climatic conditions, could impact tropospheric ozone in different ways: A higher leaf area index of the vegetation would enhance dry deposition of ozone (Fu and Tai, 2015). In low NO_x regions enhanced emissions of isoprene emitting species could decrease ozone concentrations, while they would lead to an ozone increase in high NO_x regions (Fu and Tai, 2015).

Traditionally, the risk of ozone damage to plants is estimated on the basis of the accumulated ozone exposure above 40 ppbv (AOT 40) (Felzer et al., 2005). However, the negative effects of ozone on vegetation are have been observed to be more closely related to the effective dose, i.e. the stomatal flux × time minus the portion of ozone which can be detoxicated by the plant defence system (Massman, 2004).

Accurate In the expected CO_2 richer and warmer future atmosphere (IPCC, 2013), plants may reduce stomatal conductance and thus indirectly alleviate ozone damage (Sitch et al., 2007). However, accurate experimental quantification of the stomatal uptake of ozone is complicated by the presence of other ozone sinks, either in the gas phase or on the plant surface (Fruekilde et al., 1998; Cape et al., 2009). In previous studies the ozone flux through the stomata was calculated by multiplying the stomatal ozone conductance with the ambient ozone concentration (Kurpius and Goldstein, 2003; Cieslik, 2004; Goldstein et al., 2004; Fares et al., 2012)(see e.g. Kurpius and Goldstein, 2003; Cieslik, 2004; Goldstein et al., 2004; Fares et al., 2012), assuming similar gradient profiles of ozone and H_2O close to the stomata. As we will show, in the case of for ozone-reactive leaf surfaces this approach is not correct and leads fully correct and may lead to an overestimation of stomatal ozone uptake in the case of very reactive surfaces.

We present results from ozone fumigation experiments, in which intact leaves of different varieties of tobacco (*Nicotiana tabacum*) were exposed to elevated ozone levels (20–150 ppbv) under light and dark conditions in an exceptionally clean plant enclosure system (see Materials and methods section for experimental details). The *Nicotiana tabacum* species is famous for large differences in the ozone tolerance of the different varieties. For example, the *Bel W3* is known to be very ozone sensitive (Heggestad, 1991; Loreto et al., 2001) and has therefore been used as an ozone indicator plant in earlier times (see Heggestad, 1991, and references therein). Conversely, the *Bel B* variety is known to be non-sensitive (Heggestad, 1991). The high ozone tolerance of this variety has been attributed to wider epidermal cells and more spongy mesophyll cell layers (Borowiak et al., 2010) and to differences in the plant's ability to cope with oxidative stress once ozone has entered the stomata (Schraudner et al., 1998; Eltayeb et al., 2007).

Several studies were investigating the possibility to increase the ozone tolerance of plants by external application of ozone-scavenging compounds (Gilbert et al., 1977; Loreto et al., 2001; Vickers et al., 2009a; Singh and Agrawal, 2010; Agathokleous et al., 2014) or by enabling the emission of volatile terpenoids in transgenic plants (Vickers et al., 2009b; Palmer-Young et al., 2015). We show here that some of the tobacco varieties investigated in our experiments are intrinsically equipped with ozone scavenging compounds located on their leaf cuticula. As is the case for many other plant species (Fahn, 1988), tobacco leaves possess glandular trichomes. In tobacco, various diterpenoids are the major compounds exuded by these secretory structures at the leaf surface (Sallaud et al., 2012). The exudates cover the plant leaves as a defence barrier, for example against arthropod pests (Wagner, 1991; Lin and Wagner, 1994); they were shown to have an anti-fungal (Kennedy et al., 1992) and insecticidal action (Kennedy et al., 1995). We show that in a tobacco variety secreting the diterpenoid *cis*-abienolalso has a very , the exudates have a beneficial side-effect: they act as a powerful chemical protection shield against stomatal ozone uptake due to ozone depletion at its by depleting ozone at the leaf surface.

Surface-assisted ozonolysis not only protects plants from uptake of phytotoxic ozone through stomata, but also acts as a source of volatile carbonyls into the atmosphere, impacting atmospheric chemistry. To our knowledge, our study reports for the first time on detailed measurements of plant surface-assisted ozonolysis of semi-volatile diterpenoids forming volatile carbonyl products.

2 Materials and methods

2.1 Plant material

We used the following four tobacco cultivars: *Ambalema*, secreting only the diterpenoid *cis*-abienol ($C_{20}H_{34}O$, see Fig. 1), *BYBA* secreting α- and β-cembratrien-diols (CBTdiols, $C_{20}H_{34}O_2$, see Fig. 1) and *Basma Drama*, secreting all these compounds (Sallaud et al., 2012). The new 3H02 line does not exude diterpenoids at all (see Appendix A).

Seeds of the tobacco cultivars were obtained from the Leibniz Institute of Plant Biochemistry, Department of Cell and Metabolic Biology, Halle. The plants were grown in the green houses of the Institute of Ecology of the University of Innsbruck for 8–10 weeks in standard soil.

Before being used in the experiments the sample plants were allowed to adapt 1–4 weeks in the laboratory, obtaining light from the same true light lamp type as used during the measurements (see Setup section).

Plants were installed into the plant enclosure used for ozone fumigation the evening before the actual experiment, so they could adapt to the system and recover from possible stress during installation. The (single-sided) leaf area enclosed was typically in the range of 250–850. The sample plants were well watered and in a good physiological condition (fluxes during dark and light conditions are given in Table S1 in the Supplement) and showed no visible signs of damage. At the beginning of the experiments, when no ozone was added, no significant stress signals in form of green leaf volatiles were detected.

In total, combined dark and light ozone fumigation experiments were conducted with five *Ambalema*, two *Basma Drama*, one *BYBA* and three 3H02 samples. Moreover, experiments under solely light conditions were conducted with eight *Ambalema*, four *Basma Drama*, four *BYBA* and two 3H02 plants. Each sample plant was tested only once.

2.2 Setup

In the present ozone experiments we used only inert materials such as Teflon®, PEEK® or Duran® glass in order to minimise artificial side-reactions of ozone with unsaturated compounds, present in e.g. sealing materials like rubber. Moreover, special care was taken to avoid fingerprints, which could result in side reactions of ozone with skin oils (Wisthaler and Weschler, 2010). Ozone loss, estimated from measured ozone concentrations at the inlet and outlet of the empty plant enclosure, was typically less than $5\,\%$.

For plant fumigation, synthetic air 5.0 grade was mixed with CO_2 4.8 grade (both Messer Austria GmbH, Gumpoldskirchen, Austria). By bubbling the air in distilled water and passing it by a subsequent thermoelectric cooler (TEC) the relative humidity was set. Before entering the plant enclosure, the air was flushed through an ozone generator (UVP, Upland (CA), USA). The enclosure system consisted of a desiccator (Schott Duran®) of 17.3 L volume, turned upside-down, and two end-matched PTFE® ground plates. A central hole served as feed-through for the plant stem, possible gaps were sealed with Teflon® tape. The (single-sided) leaf area enclosed was typically in the range of 250–850 cm^2.

An ozone detector (Model 49i, Thermo Fisher Scientific Inc. Franklin (MA), USA) and an infrared gas analyser (LI-840A CO_2/H_2O Analyzer, LI-COR® inc., Lincoln (NE), USA) were sampling at 2 min intervals from either the inlet or outlet of the enclosure. Plant enclosure inlet ozone concentrations were typically kept constant throughout each experiment and were adjusted to obtain realistic ambient ozone concentrations at the enclosure outlet during light conditions (e.g. ~ 60 ppbv in Fig. 3). Relative humidity in the plant enclosure ranged from typically $\sim 55\,\%$ in dark experiments up to $\sim 95\,\%$ in light experiments.

VOC were quantitatively detected at the enclosure outlet by a Selective Reagent Ionization Time-of-Flight Mass Spectrometer (SRI-ToF-MS, see next section) which was switched every 6 min between H_3O^+ and NO^+ reagent ion mode.

Sample plants were illuminated by a true light lamp (Dakar, MT/HQI-T/D, Lanzini Illuminazione, Brescia, Italy). Infra-red light was shielded off by a continuously flushed water bath in order to prevent heating of the plant enclosure. Photosynthetically active radiation (PAR) was measured with a sunshine sensor (model BF3, Delta T Devices Ltd, Cambridge, UK) and temperature on the outer plant enclosure surface with K-type thermocouples.

2.3 SRI-ToF-MS

The UIBK Advanced SRI-ToF-MS (University of Innsbruck Advanced Selective Reagent Ionization Time-of-Flight Mass Spectrometer, Breitenlechner and Hansel, 2015) combines the high mass resolution of PTR-ToF-MS (Graus et al., 2010) with the capability to separate isomeric compounds having specific functional groups. For this purpose, the SRI-ToF-MS makes use of different chemical ionization pathways of a set of fast switchable primary ions (here: H_3O^+ and NO^+). Moreover, the employment of different primary ions could help to differentiate molecules suffering from fragmentation onto the same mass to charge ratio in the standard H_3O^+ mode (Karl et al., 2012).

Examples of differentiable isomers are aldehydes and ketones. In the H_3O^+ reagent ion mode, aldehydes and ketones both exhibit proton transfer and thus e.g. methyl vinyl ketone (MVK) and methacrolein (MACR) are both detected as $C_4H_7O^+$ (m/z 71.050). In NO^+ reagent ion mode, most aldehydes exhibit hydride ion transfer and ketones clustering reactions, comparable to the ionization mechanisms in a SIFT instrument (Španěl et al., 1997). Thus MVK is detected as $C_4H_6O \bullet NO^+$ (m/z 100.040), whereas MACR is detected as $C_4H_5O^+$ (m/z 69.034).

In addition to isomeric separation, the high flow through the drift tube (here: $\sim 500\,\mathrm{mL\,min^{-1}}$ compared to 10–20 $\mathrm{mL\,min^{-1}}$ in a standard instrument) allows for the first time the detection of semi-volatile compounds such as the diterpenoid *cis*-abienol ($C_{20}H_{34}O$).

The SRI-ToF-MS was operated under standard conditions, 60 °C drift tube temperature, 540 or 350 V drift voltage and 2.3 mbar drift pressure, corresponding to an E/N of 120 or 78 Td (E being the electric field strength and N the gas number density; $1\,\mathrm{Td} = 10^{-17}\,\mathrm{V\,cm^2}$) in $\mathrm{H_3O^+}$ respectively or $\mathrm{NO^+}$ reagent ion mode, respectively. The instrument was calibrated approximately once a week by dynamic dilution of VOC using 2 different gas standards (Apel Riemer Environmental Inc., Broomfield (CO), USA), containing ca. 30 different VOC of different functionality distributed over the mass range of 30–204 amu. Full SRI-ToF-MS mass spectra were recorded up to m/z 315 with a 1 s time resolution. Raw data analysis was performed using the PTR-ToF Data Analyzer v3.36 and v4.17 (Müller et al., 2013).

2.4 *cis*-abienol identification

For the identification of *cis*-abienol a pure standard was acquired (Toronto Research Chemicals, Toronto, Canada). The powder was dissolved in n-hexane and applied on the surface of a glass container, which was put into the enclosure system and treated like the plant samples. In $\mathrm{H_3O^+}$ reagent ion mode, the major *cis*-abienol derived signal was detected on m/z 273.258 ($\mathrm{C_{20}H_{33}^+}$); like many other alcohols, *cis*-abienol is losing $\mathrm{H_2O}$ after the protonation reaction. Minor fragment signals in the range of a few percent were detected at m/z 191.180 ($\mathrm{C_{14}H_{23}^+}$), m/z 163.149 ($\mathrm{C_{12}H_{19}^+}$) and m/z 217.196 ($\mathrm{C_{16}H_{25}^+}$), respectively.

In $\mathrm{NO^+}$ reagent ion mode, the major *cis*-abienol derived signals were detected at m/z 272.250 ($\mathrm{C_{20}H_{32}^+}$) and m/z 178.172 ($\mathrm{C_{13}H_{22}^+}$). Minor signals were measured at m/z 163.149 ($\mathrm{C_{12}H_{19}^+}$) and m/z 134.101 ($\mathrm{C_{10}H_{14}^+}$), respectively.

Ozonolysis of the pure *cis*-abienol standard yielded the same primary ozonolysis products (see below) as in the case of *Ambalema* plants.

2.5 Leaf stripping

In order to relate the observed ozonolysis carbonyls to plant surface reactions, leaf exudates of untreated tobacco plants were stripped off by dipping leaves (of similar area) of untreated *Ambalema*, *Basma Drama* and 3H02 plants into n-hexane ($\sim 100\,\mathrm{mL}$ for $1000\,\mathrm{cm^2}$ leaf area) for ~ 1 min. The n-hexane – leaf exudate solution was then distributed as evenly as possible onto the inner surface of the empty desiccator serving as plant enclosure. n-hexane evaporated quickly and was further reduced by flushing the glass cuvette with pure synthetic air. Afterwards, ozone fumigation experiments were performed similar to the experiments with intact plants.

2.6 GC-MS analysis

Non-volatile ozonolysis products and unreacted surface compounds were analysed by GC-MS (see also Supplement). Directly after the ozone fumigation experiments we extracted leaf exudates and low volatility ozonolysis products from the fresh tobacco leaves (see Leaf Stripping section). 1 µL portions of the samples were then injected directly into a GC-MS for analysis on a 6890 N gas chromatograph coupled to a 5973 N mass spectrometer (Agilent Technologies) according to the procedures described elsewhere (Sallaud et al., 2012).

Tobacco diterpenoids were identified on the basis of their mass spectra, as described in the literature (Enzell et al., 1984).

2.7 Calculation of leaf gas exchange parameters

For the calculation of the gas exchange parameters we followed well established procedures by Caemmerer and Farquhar (1981) and Ball (1987). Transpiration rate E, assimilation rate A, total ozone flux $F_{\mathrm{tot,O_3}}$ and total water vapour conductance $g_{\mathrm{l,H_2O}}$ were calculated from

$$E = \frac{u_{\mathrm{e}}}{s} \cdot \frac{w_{\mathrm{o}} - w_{\mathrm{e}}}{1 - w_{\mathrm{o}} \cdot 10^{-3}}, \; [\mathrm{mmol\,m^{-2}\,s^{-1}}] \tag{1}$$

$$A = \frac{u_{\mathrm{e}}}{s} \cdot \left[c_{\mathrm{e}} - \left(\frac{1 - w_{\mathrm{e}} \cdot 10^{-3}}{1 - w_{\mathrm{o}} \cdot 10^{-3}} \right) \cdot c_{\mathrm{o}} \right], \; [\mathrm{µmol\,m^{-2}\,s^{-1}}] \tag{2}$$

$$F_{\mathrm{tot,O_3}} = \frac{u_{\mathrm{e}}}{s} \cdot \left[o_{\mathrm{e}} - \left(\frac{1 - w_{\mathrm{e}} \cdot 10^{-3}}{1 - w_{\mathrm{o}} \cdot 10^{-3}} \right) \cdot o_{\mathrm{o}} \right], \; [\mathrm{nmol\,m^{-2}\,s^{-1}}] \tag{3}$$

$$g_{\mathrm{l,H_2O}} = \frac{10^3 \cdot E \left(1 - \frac{w_{\mathrm{o}} + w_{\mathrm{i}}}{2 \cdot 10^3}\right)}{w_{\mathrm{i}} - w_{\mathrm{o}}}, \; [\mathrm{mmol\,m^{-2}\,s^{-1}}] \tag{4}$$

with u_{e} the molar flow of air entering the enclosure in $[\mathrm{mol\,s^{-1}}]$, s the leaf area in $[m^2]$, $w_{\mathrm{e}}/c_{\mathrm{e}}/o_{\mathrm{e}}$ and $w_{\mathrm{o}}/c_{\mathrm{o}}/o_{\mathrm{o}}$ the mole fraction of water vapour/$\mathrm{CO_2}$/ozone entering respectively leaving the plant enclosure in $[\mathrm{mmol\,mol^{-1}}]$, $[\mathrm{µmol\,mol^{-1}}]$ and $[\mathrm{nmol\,mol^{-1}}]$, respectively. w_{i} is the mole fraction of water vapour inside the leaf in $[\mathrm{mmol\,mol^{-1}}]$ and is typically assumed to be the saturation mole fraction at leaf temperature (Ball, 1987).

For the calculation of the total ozone conductance we applied a ternary diffusion model as has been proposed by Caemmerer and Farquhar (1981). Thereby, pairwise interactions between ozone, water vapour and air are considered (for the sake of simplicity we neglected interactions with $\mathrm{CO_2}$). Interactions of ozone molecules with water vapour are important only for that portion of ozone, which is entering the stomatal pores and not for that lost in reactions at the leaf surface. However, in the latter case the consideration of binary diffusion between ozone and water leads to an overestimation of the total ozone conductance in the range of $< 1\,\%$.

Total ozone conductance $g_{\mathrm{l,O_3}}$ is then defined by

$$g_{\mathrm{l,O_3}} = \frac{-10^3 \cdot F_{\mathrm{tot,O_3}} + \left(\frac{o_{\mathrm{a}} + o_{\mathrm{i}}}{2}\right) \cdot E}{o_{\mathrm{a}} - o_{\mathrm{i}}}, \; [\mathrm{mmol\,m^{-2}\,s^{-1}}] \tag{5}$$

with o_{i} and o_{a} the mole fractions of ozone inside the leaf (at the leaf surface for reactive leaf surfaces) and in the surrounding air, respectively. o_{a} equals the ozone mole fraction o_{o} measured at the outlet of the plant enclosure. Typically, we consider $o_{\mathrm{i}} \approx 0$ (Laisk et al., 1989) and therefore Eq. (5) simplifies further to

$$g_{\mathrm{l,O_3}} = \frac{-10^3 \cdot F_{\mathrm{tot,O_3}} + \frac{o_{\mathrm{a}}}{2} \cdot E}{o_{\mathrm{a}}} \tag{6}$$

2.8 Quantification of the ozone depletion capability of individual plants

In our fumigation experiments the ozone concentrations in the plant enclosure varied between the different experiments and within experiments switching from light to dark conditions. In order to compare the ozone depletion capability (i.e. surface plus stomatal sinks) of different plants or of the same plant under dark and light conditions, it is therefore important to use a concentration independent measure. As for a given ozone conductance the ozone flux increases with the ambient ozone concentration (cf. Eqs. 3+6), we follow others (see e.g. Wohlfahrt et al., 2009) and use the ozone conductance values instead. In experiments with plants having an ozone reactive surface, the total ozone conductance $g_{\mathrm{l,O_3}}$ (Eq. 6) comprises boundary layer conductance, stomatal conductance and cuticular conductance. Stomatal and boundary layer ozone conductances can be calculated from those of water vapour by correcting for the different diffusivities of the two gases. The boundary layer water vapour conductance could be determined by measuring temperature and evaporation rate from leaf models made of chromatography paper (see Ball 1987). However, in our experiments this was not really practical for all sample plants which were all complexly and differently shaped. Consequently, also the stomatal water vapour and ozone conductances could not be inferred from the calculated total water vapour conductance (Eq. 4).

As we show in the Supplement, even if stomatal and boundary layer ozone conductances are known, for semi-reactive leaf surfaces the calculation of stomatal and non-stomatal parts of the total ozone flux is not feasible.

For these reasons we report here only total ozone conductance values (Eq. 6), normalized to the single-sided leaf area or to the area of the enclosure covered with leaf exudates in experiments with pure leaf surface compounds (see Sec. 2.5).

2.9 Fluid dynamic calculations

In order to visualise the ozone concentration gradients caused by plant ozone uptake, two idealised setups were simulated: a macroscopic plant model in an ambient air flow and a microscopic model for the stomatal gas exchange. The simulations were done using the open source CFD code OpenFOAM (www.openfoam.com).

In the microscopic model the air flow was neglected and a pure diffusion process was simulated. Stomata were modelled as $100\,\mu\mathrm{m}$ long and $40\,\mu\mathrm{m}$ wide eye-shaped openings recessed $20\,\mu\mathrm{m}$ deep into the leaf surface. The simulation domain with 500 000 cells covered an area of $300\,\mu\mathrm{m}$ square around the stoma and extended 2 mm from the leaf surface into the surrounding gas. A single stoma with cyclic boundaries was used to represent a whole leaf with stomata spread repeatedly over its surface. The ozone-reactive bottom of the stomata was modelled as $100\,\%$ efficient sink (Laisk et al., 1989) with a constant ozone concentration of zero, while the side walls of the stomata were assumed not to absorb ozone and set to zero gradient. The top of the measurement domain acting as ozone inlet from the surrounding was set to one. The leaf surface around the stomata was set to zero gradient or to a fixed concentration of zero, representing two idealised plant types with either non-reactive or reactive leaf surface. “scalarTransportFoam” was run on this grid with a uniform zero velocity field until a steady state was reached.

For the macroscopic model (see Supplement) a laminar flow around the plant was simulated using the steady state Reynolds averaged Navier–Stokes solver “simpleFoam”, the transport of ozone in the resulting flow velocity field was studied using the “scalarTransportFoam” solver. The simulated gas volume consisted of a cube with 20 cm edge length with the shape of an exemplary tobacco plant cut out of its volume (see Fig. S4S3). The resulting simulation domain was divided into a hexahedron-dominant grid of 3.7 million cells with the finest granularity around the stomata and the leaf surfaces with the OpenFOAM tool “snappyHexMesh”. The domain was divided into eight subdomains for parallel computation. Stomata were represented by small patches spread equally over the leaf surfaces, covering $10\,\%$ of the total leaf area. The boundary conditions for the gas flow simulation consisted of an inlet with $2\,\mathrm{mm\,s^{-1}}$ velocity entering on one face of the cube and a constant pressure boundary condition outlet on the opposite face. The gas velocity on the plant surface was set to zero. Initial conditions for the flow simulation were calculated with “potentialFoam” to speed up convergence of the “simpleFoam” solver. The simulation was run until the flow velocity field reached a steady state. For the diffusion calculations a relative initial concentration of ozone was set to one at the inlet and to zero on the stomata patches. Like in the microscopic model calculations, the leaf surface was either a zero concentration gradient boundary (for an idealised 3H02 plant type) or a fixed concentration value of zero (for an idealised *Ambalema* plant type). In the previously calculated velocity field the ozone transport was simulated until a steady state was reached, too.

3 Results and discussion

3.1 Detected oxidation products from plant surface Expected ozonolysis products of diterpenoids *cis*-abienol and cembratrien-diols

We observed a prompt release of volatile carbonyls as soon as tobacco leaves were fumigated with ozone. The *Ambalema* and *Basma Drama* varieties released methyl vinyl ketone (MVK,) and formaldehyde (). These compounds are produced by surface-assisted ozonolysis of *cis*-abienol (see Figs. 1 and 3), a Apart from the 3H02 variety, the investigated tobacco varieties secrete different unsaturated diterpenoids (see Sec. 2.1). According to the Criegee mechanism (Criegee, 1975), ozone attacks the carbon double bonds of alkenes forming primary carboyls and so-called Criegee Intermediates (see Supplement). Criegee Intermediates are, however, expected to be too short-lived to be detected directly by the instruments used in our experiments (see Supplement). We were therefore interested primarily in the stable, volatile ozonolysis carbonyls, which could be detected in real-time by our SRI-ToF-MS.

For the semi-volatile diterpenoid with two exocyclic double bonds . MVK was detected at m/z71.050 () and m/z100.040 (•)in the respectively reagent ion mode of the SRI-ToF-MS. Formaldehyde was detected only using as reagent ion at m/z31.018 (), taking into account the humidity dependent sensitivity (Hansel et al., 1997). In the reagent ion mode formaldehyde can not be ionized (Španěl et al., 1997), consequently we detected no signal.

In addition, we detected sclaral, a non-volatile compound, in surface extracts obtained from fumigated diterpenoid *cis*-abienol with two exocyclic double bonds, exuded by the *Ambalema* and *Basma Drama* plants (see Materials and methods and Supplement) . Sclaral is an isomerisation product of the carbonyl formed in *cis*-abienol ozonolysis (cf. varieties, we expected the formation of formaldehyde (HCHO) and methyl vinyl ketone (MVK, C_4H_6O, see Fig. 1).

In the case of the ring structured CBTdiols with three endocyclic double bonds, produced by the *Basma Drama* and *BYBA* plants, at least two ozonolysis steps are needed to form volatile carbonyls(see Fig. 1). The most volatile ozonolysis product – 4-oxopentanal () – was detected by SRI-ToF-MS in the gas phase at m/z101.060 () in and m/z99.045 () in reagent ion mode, respectively.

According to the Criegee mechanism (Criegee, 1975), along with the carbonyls, Criegee Intermediates are also formed in ozonolysis reactions.However, they are expected to be too short-lived to be directly detected by the instruments used in our experiments (see Supplement) .

3.2 Separation of ozone surface and gas phase reactions

The semi-volatile diterpenoids exuded by the tobacco varieties could also react with ozone in the gas phase. However, it is unlikely that gas phase reactions played a major role in our experiments. The air in the enclosure system was exchanged every $\sim$ 5min. Therefore only extremely fast gas phase ozone – alkene reactions have to be considered. For an ozone concentration of 100ppbv, a reaction rate of 1.35×10^{-15}results in an alkene ozonolysis lifetime of 5min. Such fast ozonolysis rates have only been measured for a few very reactive sesquiterpenes (Atkinson and Arey, 2003). We found no reaction rates of *cis*-abienol and CBTdiols with ozone in the literature to exclude the possibility of a gas phase contribution to total ozone loss in our experiments a priori. Nonetheless, taking into account the estimated vapour pressures of *cis*-abienol ($\sim 10^{-9}$bar) and CBTdiol ($\sim 10^{-12}$bar) (Goldstein and Galbally, 2007) we can state that the bulk of the exuded diterpenoids stayed at the leaf surface and that other surfaces (e.g. the inner surface of the plant enclosure and the tubing system) were very slowly covered by condensed diterpenoids. This is also the explanation for the bursts of volatile ozonolysis products at the beginning of every ozone fumigation (see e.g. Fig. 3). Diterpenoids were deposited on all surfaces during plant acclimation under ozone free conditions lasting for several hours (see also Supplement).

In order to assess the significance of gas phase ozonolysis to our results, we connected the plant enclosure containing a diterpenoid emitting tobacco plant with a second empty enclosure downstream and added ozone only to the second enclosure. Only negligible carbonyl signals were observed once the initial burst from deposited diterpenoids faded away (see Supplement and Fig. S1)three smallest carbonyl products are shown in Fig. 1, whereby 4-oxopentanal ($C_5H_8O_2$) is expected to be the most volatile one (Goldstein and Galbally, 2007).

3.2 Ozonolysis of Ozone fumigation experiments with **pure leaf surface compounds**

In order to relate the a release of carbonyls to surface chemistry only and to exclude stimulated emissions caused, e.g. by the plant ozone defence system, we investigated ozone reactions with pure leaf surface compounds. Leaf extracts were extracts. Leaf surface compounds were extracted with n-hexane and subsequently applied onto the inner surface of an empty plant enclosure and fumigated with ozone the usual way (see Materials and methods section).

Ambalema leaf extracts showed a weak signal of *cis*-abienol- abienol (we refer to the Materials and methods section for the identification of this compound), which disappeared during ozone fumigation while MVK and formaldehyde were prominently observed. The These carbonyls are produced by surface-assisted ozonolysis of *Basma Drama*cisextracts showed MVK , -abienol (see Fig. 1). MVK was detected at m/z 71.050 ($C_4H_7O^+$) and m/z 100.040 ($C_4H_6O \bullet NO^+$) in the H_3O^+ respectively NO^+ reagent ion mode of the SRI-ToF-MS. Formaldehyde was detected only using H_3O^+ as reagent ion at m/z 31.018 (CH_3O^+), taking into account the humidity dependent sensitivity (Hansel et al., 1997). In the NO^+ reagent ion mode formaldehyde cannot be ionized (Španěl et al., 1997), consequently we detected no signal.

In the ozone fumigation experiments using *Basma Drama* leaf extracts, besides MVK and formaldehyde and 4-oxopentanal as ozonolysis products from of *cis*-abienoland CBTdiols as expected., also the most volatile CBTdiol ozonolysis product – 4-oxopentanal – was detected in the gas phase by SRI-ToF-MS. 4-oxopentanal was detected at m/z 101.060 ($C_5H_9O_2^+$) in H_3O^+ and m/z 99.045 ($C_5H_7O_2^+$) in NO^+reagent ion mode, respectively.

No significant amount of volatile carbonyls was observed from ozonolysis of 3H02 leaf extracts. Consistently, the total ozone conductance g_{1,O_3} – a measure of the rate of ozone depleted at the surface – was far higher was far less than in experiments with extracts from diterpenoid-exuding tobacco varieties (see Fig. 2). This is in line with the results from the corresponding experiments with intact plants .

While the (see below). The ozone depletion efficiency of the 3H02 exudates was decreasing fast, while the presence of *cis*-abienol in *Ambalema* leaf exudates kept the ozone conductance at elevated levels for many hours (cf. Fig. 2). On fresh leaves of

3.3 Ozone fumigation experiments with diterpenoid exuding tobacco varieties

Also in experiments with intact plants we observed a prompt release of volatile carbonyls as soon as the tobacco leaves were fumigated with ozone. The *Ambalema* and *Basma Drama* varieties released MVK and formaldehyde. In addition, we detected sclaral, a non-volatile compound, in surface extracts obtained from ozone fumigated plants of the same varieties (see Materials and methods and Supplement). Sclaral is an isomerisation product of the C_{16} carbonyl formed in *cis*-abienol ozonolysis (cf. Fig. 1). All these compounds can therefore be attributed again to surface-assisted ozonolysis of *cis*-abienol (see Fig. 1).

In experiments using *Basma Drama* and *BYBA* plants we detected the CBTdiol ozonolysis product 4-oxopentanal, similar to the ozone fumigation experiments with leaf surface extracts (see previous section).

Figure 3 shows a typical result of an ozonolysis experiment using *Ambalema* plants. Immediately after starting the ozone fumigation, the *cis*-abienol signal decreased, while initial bursts of MVK and formaldehyde were detected. These initial bursts can be attributed to surface ozonolysis of *cis*-abienol deposited on *all* surfaces (i.e. surfaces of the whole plant, the enclosure and the enclosure outlet tubing) during plant acclimatisation under ozone free conditions lasting $> 12\,h$ (see Sec. 3.5 and Supplement).

In plant experiments using diterpenoid exuding tobacco varieties, the carbonyl emission and consequently the total ozone conductance and flux (under constant light) eventually reached a steady state, when the diterpenoid production by the trichomes (leading to a permanent deposition of those onto the plant surface) and plant surface reactions were in equilibrium . (cf. Fig. 3). This is in contrast to experiments with pure leaf surface compounds, in which the diterpenoids were slowly consumed as ozone fumigation progressed (see Sec. 3.2).

Simulating diurnal ozone variations over two days in experiments with *Ambalema* and *Basma Drama* plants, we could show that the reactive layer at the plant surface is a large pool and not quickly consumed (see Supplement and Fig. S2). We therefore assume that the diterpenoids released are likely to represent a long term ozone protection for these varieties.

3.4 Variety specific ozone depletion during dark and light phases

In order to have a measure of further experiments we investigated the ozone depletion capability of the various plants, the individual total ozone conductance g_{1,O_3} was calculated (Caemmerer and Farquhar, 1981). At this point, g_{1,O_3} is a measure of the rate of ozone depleted at the surface and within the stomata.

by different tobacco varieties under dark and light conditions.

In dark experiments, when stomatal pores are almost closed, the *Ambalema* variety showed the highest total ozone conductance under steady-state conditions (cf. Fig. 4a). This is a direct indication for the high ozone depletion capacity of the surface of this variety.

Due to the lack of reactive diterpenoids on the leaf surface of 3H02 plants, the surface ozone sink plays a minor role for this tobacco line. However, we cannot totally exclude the presence of other unsaturated compounds at the surface of this tobacco line.

variety.

The low surface reactivity of the *Basma Drama* and *BYBA* varieties correlates with the lower amount of detected ozonolysis carbonyls compared to that of the *Ambalema* variety in dark conditions. This might be related to a lower diterpenoid surface coverage of these two varieties and the expected lower reactivity of the CBTdiols having endocyclic double bonds (Atkinson and Arey, 2003).

In a further step we investigated the change in total ozone conductanceof different tobacco varieties when The *Ambalema* variety also shows a higher $g_{\mathrm{l,H_2O}}$ and dark respiration than the other varieties (cf. Fig. 4b+c). $g_{\mathrm{l,H_2O}}$ linearly correlates with the stomatal water vapour conductance and therefore also with the stomatal ozone conductance. However, higher stomatal conductance during dark conditions cannot explain the large differences in $g_{\mathrm{l,O_3}}$ between the plant types. While $g_{\mathrm{l,H_2O}}$ of the Ambalema variety in dark conditions is about twice as high as that of the 3H02 variety, the corresponding $g_{\mathrm{l,O_3}}$ is four times as high.

When switching from dark to light conditions , thereby increasing stomatal conductance and thus stomatal ozone flux. Ozone entering the stomata is believed to be completely degraded (Laisk et al., 1989)we assume cuticular conductance not to change significantly and thus an increase in the calculated $g_{\mathrm{l,O_3}}$ is attributable mainly to an increasing stomatal ozone conductance. In the case of *Ambalema*, switching the light on increased the total conductance by $\sim 55\,\%$ (see Fig. 4). In contrast, in the 3H02 case, switching on the light triggered a dramatic an substantial increase in the total ozone conductance by $\sim 340\,\%$ (cf. Fig. 4). During light conditions the total ozone conductances of the different tobacco varieties were in a comparable range; slightly higher values were observed for the diterpenoid exuding lines *Ambalema*, *Basma Drama* and *BYBA*.

3.5 Separation of ozone surface and gas phase reactions

In order to qualify the measured total ozone fluxes for the calculation of $g_{\mathrm{l,O_3}}$ values, we had to take into account the possibility of homogeneous gas phase ozonolysis of the semi-volatile diterpenoids exuded by the tobacco varieties.

To assess the significance of gas phase ozonolysis to our results, we connected the plant enclosure containing a diterpenoid emitting tobacco plant with a second empty enclosure downstream and added ozone only to the second enclosure. Only negligible carbonyl signals were observed once the initial burst from deposited diterpenoids faded away (see Supplement and Fig. S1). This result indicates that with our setup gas-phase reactions of the diterpenoids were not significant.

This observation can be explained theoretically, too. The air in our enclosure system was exchanged every ~ 5 min. Therefore, only extremely fast gas phase ozone – alkene reactions have to be considered. For an ozone concentration of 100 ppbv, a reaction rate of $1.35\times10^{-15}\,\mathrm{cm^3\,s^{-1}}$ results in an alkene ozonolysis lifetime of 5 min. Such fast ozonolysis rates have only been measured for a few very reactive sesquiterpenes (Atkinson and Arey, 2003). We found no reaction rates of *cis*-abienol and CBTdiols with ozone in the literature to exclude the possibility of a gas phase contribution to total ozone loss in our experiments a priori. Nonetheless, taking into account the estimated vapour pressures of *cis*-abienol ($\sim 10^{-9}$ bar) and CBTdiol ($\sim 10^{-12}$ bar) (Goldstein and Galbally, 2007) we can state that the bulk of the exuded diterpenoids stayed at the leaf surface and that other surfaces (e.g. the inner surface of the plant enclosure and the tubing system) were very slowly covered by condensed diterpenoids. This is also the explanation for the bursts of volatile ozonolysis products at the beginning of every ozone fumigation (see e.g. Fig. 3). We therefore assume that gas phase reactions are unlikely to have played a major role in our experiments.

3.6 Fluid dynamic model calculations

Computational fluid dynamics Microscopic fluid dynamic model calculations (see Materials and methods) revealed the principles responsible for this the strong variety-dependent partitioning between stomatal and non-stomatal ozone loss (see Sct. 3.4). The mixed convective and diffusive ozone transport from the surrounding atmosphere to the plant surface and into the stomata was simulated for two idealised plant types under light conditions when the leaf stomata are open. The stomatal pores were exemplarily modelled as small patches uniformly spread over the entire leaf surface. For one model plant we assumed stomatal ozone uptake only, corresponding to an idealised 3H02 variety plant lacking any reactive surface compounds. The second model plant was representing an idealised *Ambalema* variety. The surface acted as a perfect ozone sink with every ozone molecule reaching it being lost, either on the leaf surface or through the stomata.

Figure 5a and b show the resistance schemes used to describe the ozone flux to the leaves in the two scenarios, which were the basis for our simulations. Ambient ozone has to overcome the boundary layer resistance R_b and the stomatal resistance R_s before being destroyed in the stomatal cavity (for the sake of simplicity we neglected here the mesophyl resistance, which comprises diffusion through inner air spaces and dissolution of the gas in the cell wall water, followed by losses in the aqueous phase, penetration of plasmalemma or chemical reactions in the cell, cf. Neubert et al., 1993). In the case of a non-reactive leaf surface, ozone depletion within the stomata is the sole ozone sink (see Fig. 5a).

In the case of an ozone-reactive leaf surface, an additional surface chemical resistance R_sc has to be introduced, which is parallel to the stomatal resistance (see Fig. 5b). R_sc inversely correlates with the reactive uptake coefficient of ozone at the leaf surface. In the case of the model plant having a non-reactive surface, R_sc is very large ($R_\mathrm{sc} \to \infty$) and ozone flux to the leaf surface can be omitted. Conversely, R_sc is small for reactive surfaces.

The porous leaf surface architecture has special relevance for the gas uptake of plants. For gases having a negligible leaf surface sink (or source) – like e.g. CO_2 – steep concentration gradients parallel and perpendicular to the surface develop in close proximity to the stomata. These gradients enhance the gas transport in the diffusive leaf boundary layer towards the pores. This effect is extensively described in the literature as the "paradox of pores" (see e.g. Monson and Baldocchi, 2014). It enables plants to effectively harvest CO_2 for photosynthesis, but in the same manner also "funnels" phytotoxic ozone through the stomata into the plant leaves (see Fig. 5c).

In the case of an ozone-reactive leaf surface, R_sc is small compared to R_s and only surface-parallel ozone concentration isosurfaces develop (black lines in Fig. 5d). Concentration gradients (white lines) close to the stomata are exclusively perpendicular to the surface. Consequently, the ozone transport in the diffusive leaf boundary layer is equally distributed over the whole leaf surface and the ozone concentration in this layer is strongly reduced (see Fig. 5d). Similarly, also macroscopic model calculations show that this effect broadens the space of reduced ozone concentrations surrounding a plant with opened stomata (see Supplement and Fig. S3).

The surface-parallel concentration isosurfaces are also the reason why we can use the same reference concentration $c_{\mathrm{b,\,r}}$ for both stomatal and the stomatal and the surface chemical resistance, (cf. Fig. 5b). However, this approach does only hold if the leaf surface is a complete ozone sink (see Supplement and Fig. S3S4).

The different ozone concentration patterns in the two modelled scenarios have important implications for the stomatal ozone uptake. Typically, the stomatal conductance of ozone $g_{\mathrm{s,O_3}}$ is estimated from that of water $g_{\mathrm{s,H_2O}}$, by correcting for the different diffusivity of the two gases (see e.g. Neubert et al., 1993Ball, 1987; Neubert et al., 1993). The stomatal ozone flux $F_{\mathrm{s,O_3}}$ can then be calculated with the following formula:

$$F_{\mathrm{s,O_3}} = g_{\mathrm{s,O_3}} \cdot (c_{\mathrm{i,O_3}} - c_{\mathrm{b,O_3}}) \qquad (7)$$

with $c_{\mathrm{i,O_3}}$ being the ozone concentration in the leaf intercellular space and $c_{\mathrm{b,O_3}}$ the ozone concentration in the leaf boundary layer. For high ambient ozone concentrations $c_{\mathrm{i,O_3}}$ is typically was found to be positive (Moldau and Bichele, 2002; Loreto and Fares, 2007), but typically it is assumed to be close to zero (Laisk et al., 1989). Therefore, Eq. (7) simplifies to

$$F_{\mathrm{s,O_3}} = -g_{\mathrm{s,O_3}} \cdot c_{\mathrm{b,O_3}} \qquad (8)$$

If now surface reactions drastically reduce $c_{\mathrm{b,O_3}}$ (cf. Fig. 5b+d), the effective stomatal ozone flux is reduced, too (unless extremely turbulent air conditions prevent the formation of an ozone depleted leaf boundary layer). Thereforeand with that the effective ozone dose are also reduced, which eventually determine the phytotoxic effects of ozone to plants (Massman, 2004). At this point, it is important to note that the uptake of non surface-reactive gases such as $\mathrm{CO_2}$ is not affected by the altered ozone gradients. Thus, whenever surface loss plays a role, both surface and stomatal ozone uptake by plants have to be considered together. Previous studies might therefore have overestimated stomatal ozone uptake (e.g. Kurpius and Goldstein, 2003; Cieslik, 2004; Goldstein et al., 2004; Fares et al., 2012). Hence, their reported stomatal ozone flux values should be considered as upper limits.

It In future studies investigating the ozone depositions to vegetation, it might be worth to analyse also the surface composition of the plants. If the surfaces are covered with substantial amounts of unsaturated organic compounds, surface loss has to be considered right from the beginning in order not to overestimate stomatal ozone uptake. Due to the fact that surface reactions reduce ozone concentrations in the leaf boundary layer, it is not correct to calculate stomatal ozone loss applying the resistance scheme shown in Fig. 5a and to eventually define the surface loss of ozone as that portion of the total loss which is not explainable by gas phase reactions and stomatal uptake. Due to the fact that surface reactions reduce $c_{\mathrm{b,O_3}}$, surface loss has to be considered right from the beginning in order not to overestimate stomatal ozone uptake.

For obvious reasons this surface effect also has a consequence on the effective ozone dose which actually determines the phytotoxic effects of ozone (Massman, 2004). At this point, it is important to note that the uptake of non surface-reactive gases such as is not affected by real plants the altered ozone gradients.

For real plants this surface effect gradient profile shown in Fig. 5d is less pronounced depending on stomata depth, which reduces the total stomatal uptake, and reactive surface compounds, which show smaller surface reaction rates than assumed for the idealised $100\,\%$ efficient ozone depleting surface (see Supplement). On the contrary, plants will hardly lack any reactive surface compounds, which explains why we observed a little ozone uptake during dark conditions also for the 3H02variety, which has no significant diterpenoid emissions (cf. In the case of such a semi-reactive leaf surfaces a more sophisticated resistance scheme has to be used, which strongly complicates the calculation of stomatal and non-stomatal ozone fluxes (see Supplement and Fig. 4S4). Nonetheless, the simulations explain the experimentally observed behavior behaviour of different tobacco plants very well.

3.7 Atmospheric implications

Our results also have relevance for other ozone-initiated processes that occur in the outdoor environment. Semi-volatile, unsaturated organic species are common on various surfaces including soil with plant litter, aerosols, sea surface layers, man-made structures and plant surfaces. These are therefore potential sources of oxygenated VOC in ozone rich regions.

Resins, e.g. found at the surface of coniferous trees, Large downward ozone fluxes (Kurpius and Goldstein, 2003; Goldstein et al., 2004) and high levels of oxidized VOC (Holzinger et al., 2005) have been taken as evidence for “unconventional in-canopy chemistry” of unknown precursors in a pine forest site. We speculate that to a certain extent these unknown precursors could be reactive compounds emitted or deposited onto the vegetation surfaces. Most recent results support this speculation. A large number of compounds with diterpenoid backbones were recently observed for the first time in a different pine forest site during the BEACHON-RoMBAS campaign 2011 (Chan et al., 2015). These unsaturated diterpenoids contain the same backbone as abietic acid, a primary component of resin acids. The observed temporal variations in concentrations were similar to those of sesquiterpernoids, suggesting they are directly emitted from the local vegetation.

Resins contain high amounts of sesqui-, di- and triterpenoid compounds (Langenheim, 2003); triterpenoids (Dell and McComb, 1979; Langenheim, 2003); di- and triterpenoids are also a known constituent known constituents of surface waxes (Thimmappa et al., 2014).All these compound (Estell et al., 1994a, b; Altimir et al., 2008; Thimmappa et al., 2014). Moreover, it is estimated that about $30\,\%$ of vascular plants have glandular trichomes, which often exude higher terpenoid compounds, too (Wagner et al., 2004).

All these terpenoid classes contain carbon-carbon double bonds and are therefore reactive with O_3, OH and NO_3. Our results support the speculation that reaction rates of ozone with semi-volatiles adsorbed at the surfaces are far higher than corresponding gas-phase ozonolysis rates. Thus, the fraction of volatile carbonyls produced in surface assisted ozonolysis of adsorbed semi-volatiles could compete with their respective gas-phase production rate from OH chemistry. To some extend this source of carbonyls in form of exudates or resins at the surface of particular plants might be obscured by the immediate uptake of the volatile ozonolysis products by the plants themselves (Karl et al., 2010; Niinemets et al., 2014). ozone.This could Reactive surface compounds might also contribute to the varying ozone sensitivity of different conifer species (Schnitzler et al., 1999; Landolt et al., 2000) when exposed to the same cumulative ozone concentrations under light conditions. We anticipate therefore that surface ozonolysis plays an important role for the ozone tolerance of certain conifer species, too. Preliminary experiments with Norway spruce and Scots pine indeed point in this direction. However, due to the vast variety of different terpenoids present at the surface of these species , the assignment of observed ozonolysis products to specific precursor compounds represents a challenge.

Additional support that surface ozonolysis might also be an important source of oxygenated VOC comes from field observations. Large downward ozone fluxes (Kurpius and Goldstein, 2003; Goldstein et al., 2004) and high levels of oxidized VOC (Holzinger et al., 2005) have been taken as evidence for "unconventional in-canopy chemistry" of unknown precursors in forest sitesOur results also have relevance for other ozone-initiated processes that occur in the indoor and outdoor environment. Semi-volatile, unsaturated organic species are common on various surfaces including soil with plant litter (Weiss, 2000; Isidorov et al., 2003; Ormeño et al., 2009), aerosols (Rogge et al., 1993; D'Anna et al., 2009; Baduel et al., 2011), man-made structures (Wisthaler et al., 2005; Weschler et al., 2007; Shi and Zhao, 2015) and plant surfaces (Dell and McComb, 1979; Langenheim, 1994). These are therefore potential ozone sinks and sources of oxygenated VOC in ozone rich environments (see e.g. Wisthaler et al., 2005; Weschler et al., 2007; D'Anna et al., 2009; Baduel et al., 2011).

4 Conclusions

Our results reveal for the first time a powerful ozone protection mechanism of plants which having an ozone reactive leaf surface. This opportunistic defence mechanism, which is a beneficial side effect of semi-volatile terpenoids emitted onto the leaf surface, takes place before the phytotoxic gas enters the stomata. Plants emitting unsaturated semi-volatile compounds could have a beneficial an advantageous effect for neighbouring plants as well: either directly by reducing overall ozone concentrations (see Supplement) or indirectly through the deposition of the semi-volatile compounds onto unprotected neighbouring leaves (Schmid et al., 1992; Himanen et al., 2010; Chan et al., 2015).

Our findings have relevance not only for plants, but also for additional ozone-initiated processes that occur in the atmospheric boundary layer. The surface-assisted chemistry that we have elucidated for specific diterpenoids, linking for the first time volatile and non-volatile carbonyl products to semi-volatile precursors at the plant surface, is likely to occur also for other semi-volatile organic compounds on different surfaces(, e.g. soil with plant litter, aerosols(Rogge et al., 1993), man-made structures and even human skin, as has been shown previously , Wisthaler and Weschler, 2010). Some (Wisthaler and Weschler, 2010). We speculate that some of the ozonolysis-derived products may play important roles in atmospheric processes, influencing the budgets of OH radicals and ozone. Conversely, in our experiments we had no indication that surface ozonolysis itself releases detectable amounts of OH radicals into the gas phase (see Supplement). In order to assess the global impact of surface-assisted ozonolysis on atmospheric chemistry a more complete knowledge about the nature of reactive, semi- and low-volatility low-volatile compounds at plant surfaces as well as the mechanisms triggering their release (e.g. constitutive vs. biotic and mechanical stress induced emission) is needed.

Appendix A: Generation of the 3H02 variety – a *Nicotiana tabacum* line without diterpenoids

The *Ambalema* variety which produces only *cis*-abienol and the *Colorado* variety which produces only CBTdiols (Sallaud et al., 2012) were crossed to produce hybrid F1 plants which produce both diterpenoids. Because the genetic loci responsible for the absence of CBTdiols and the absence of *cis*-abienol are distinct and unlinked, recombinant plants which produce neither diterpenoids could be recovered by analysing the leaf surface extracts by GC-MS in the selfed progeny of the F1 plants. One of these plants was selected, propagated over 2 generations by single seed descent and named line 3H02.

Appendix B: Calculation of the total ozone conductance

For the calculation of the gas exchange parameters we followed well established procedures by Caemmerer and Farquhar (1981). Transpiration rate E, assimilation rate A and ozone fluxes $F_{\mathrm{O_3}}$ were calculated from

$$E = \frac{u_\mathrm{e}}{s} \cdot \frac{w_\mathrm{o} - w_\mathrm{e}}{1 - w_\mathrm{o}},\ [\mathrm{mmol\,(m^2\,s)^{-1}}] \tag{A1}$$

$$A = \frac{u_\mathrm{e}}{s} \cdot \left[c_\mathrm{e} - \left(\frac{1 - w_\mathrm{e}}{1 - w_\mathrm{o}}\right) \cdot c_\mathrm{o}\right],\ [\mathrm{\mu mol\,(m^2\,s)^{-1}}] \tag{A2}$$

$$F_{\mathrm{O_3}} = \frac{u_\mathrm{e}}{s} \cdot \left[o_\mathrm{e} - \left(\frac{1 - w_\mathrm{e}}{1 - w_\mathrm{o}}\right) \cdot o_\mathrm{o}\right],\ [\mathrm{nmol\,(m^2\,s)^{-1}}] \tag{A3}$$

with u_e the molar flow of air entering the enclosure, s the leaf area, $w_\mathrm{e}/c_\mathrm{e}/o_\mathrm{e}$ and $w_\mathrm{o}/c_\mathrm{o}/o_\mathrm{o}$ the mole fraction of water vapour/$\mathrm{CO_2}$/ozone entering respectively leaving the plant enclosure.

For the calculation of the total ozone conductance we applied a ternary diffusion model as has been proposed by Caemmerer and Farquhar (1981). Thereby, pairwise interactions between ozone, water vapour and air are considered (for the sake of simplicity we neglected interactions with $\mathrm{CO_2}$). Interactions of ozone molecules with water vapour are important only for that portion of ozone, which is entering the stomatal pores and not for that lost in reactions at the leaf surface. However, in the latter case the consideration of binary diffusion between ozone and water leads to an overestimation of the total ozone conductance in the range of $< 1\,\%$.

Total ozone conductance $g_{1,\mathrm{O_3}}$ is then defined by

$$g_{1,\mathrm{O_3}} = \frac{-F_{\mathrm{O_3}} + \left(\frac{o_\mathrm{a}+o_\mathrm{i}}{2}\right)\cdot E}{o_\mathrm{a} - o_\mathrm{i}}, \; [\mathrm{mmol}\,(\mathrm{m}^2\,\mathrm{s})^{-1}] \tag{A4}$$

with o_i and o_a the mole fractions of ozone inside the leaf (at the leaf surface for reactive leaf surfaces) and in the surrounding air, respectively. Typically, we consider $o_\mathrm{i} \approx 0$ (Laisk et al., 1989) and therefore Eq. (5) simplifies further to

$$g_{1,\mathrm{O_3}} = \frac{-F_{\mathrm{O_3}} + \frac{o_\mathrm{a}}{2}\cdot E}{o_\mathrm{a}} \tag{A5}$$

The Supplement related to this article is available online at doi:10.5194/acp-0-1-2015-supplement.

Acknowledgements. The authors would like to thank Francesco Loreto who initiated the tobacco experiments, Jörg-Peter (Jogi) Schnitzler for fruitful discussions and the gardeners of the Innsbruck University Botanic Gardens who grew the sample plants. W. Jud would like to thank Sheldon L. Cooper for helpful comments.

This project was financially supported by the European Science Foundation in the frame of the EuroVol MOMEVIP project and by the Austrian Fonds zur Förderung der wissenschaftlichen Forschung, project number I655-B16.

References

Agathokleous, E., Saitanis, C. J., and Papatheohari, Y.: Evaluation of Di-1-p-Menthene as Antiozonant on Bel-W3 Tobacco Plants, as Compared with Ethylenediurea, Water, Air, & Soil Pollution, 225, 2139, doi:10.1007/s11270-014-2139-y, 2014.

Altimir, N., Vesala, T., Aalto, T., Bäck, J., and Hari, P.: Stomatal-scale modelling of the competition between ozone sinks at the air-leaf interface, Tellus, Series B: Chemical and Physical Meteorology, 60 B, 381–391, doi:10.1111/j.1600-0889.2008.00344.x, 2008.

Ashmore, M. R.: Assessing the future global impacts of ozone on vegetation, Plant Cell Environ., 28, 949–964, doi:10.1111/j.1365-3040.2005.01341.x, 2005.

Atkinson, R. and Arey, J.: Atmospheric degradation of volatile organic compounds, Chem. Rev., 103, 4605–4638, doi:10.1021/cr0206420, 2003.

Baduel, C., Monge, M. E., Voisin, D., Jaffrezo, J.-L., George, C., Haddad, I. E., Marchand, N., and D'Anna, B.: Oxidation of atmospheric humic like substances by ozone: a kinetic and structural analysis approach., Environmental science & technology, 45, 5238–44, doi:10.1021/es200587z,2011.

Ball, T.: Calculations related to gas exchange, in: Stomatal Function, edited by Zeiger, E., Farquhar, G. D., and Cowan, I. R., chap. 20, pp. 445–476, Stanford University Press, Stanford, 1987.

Borowiak, K., Zbierska, J., and Drapikowska, M.: Differences in morpho-anatomical structure of ozone-sensitive and ozone-resistant tobacco cultivars, Acta Biologica Hungarica, 61, 90–100, doi:10.1556/ABiol.61.2010.1.9, 2010.

Breitenlechner, M. and Hansel, A.: Development of an Advanced Selective Reagent Ionization Time of Flight Mass Spectrometer (advanced SRI-TOF-MS), Atmos. Meas. Tech. Discuss., submitted, 2015.

Caemmerer, S. and Farquhar, G. D.: Some relationships between the biochemistry of photosynthesis and the gas exchange of leaves, Planta, 153, 376–387, doi:10.1007/BF00384257, 1981.

Cape, J. N., Hamilton, R., and Heal, M. R.: Reactive uptake of ozone at simulated leaf surfaces: implications for "non-stomatal" ozone flux, Atmos. Environ., 43, 1116–1123, doi:10.1016/j.atmosenv.2008.11.007, 2009.

Chan, A. W. H., Kreisberg, N. M., Hohaus, T., Campuzano-Jost, P., Zhao, Y., Day, D. A., Kaser, L., Karl, T., Hansel, A., Teng, A. P., Ruehl, C. R., Sueper, D. T., Jayne, J. T., Worsnop, D. R., Jimenez, J. L., Hering, S. V., and Goldstein, A. H.: Speciated measurements of semivolatile and intermediate volatility organic compounds (S/IVOCs) in a pine forest during BEACHON-RoMBAS 2011, Atmospheric Chemistry and Physics Discussions, 15, 22 331–22 377, doi:10.5194/acpd-15-22331-2015, 2015.

Cieslik, S. A.: Ozone uptake by various surface types: a comparison between dose and exposure, Atmos. Environ., 38, 2409–2420, doi:10.1016/j.atmosenv.2003.10.063, 2004.

Criegee, R.: Mechanism of ozonolysis, Angew. Chem. Int. Edit., 14, 745–752, 1975.

D'Anna, B., Jammoul, A., George, C., Stemmler, K., Fahrni, S., Ammann, M., and Wisthaler, A.: Light-induced ozone depletion by humic acid films and submicron aerosol particles, Journal of Geophysical Research, 114, D12 301, doi:10.1029/2008JD011237, 2009.

Dell, B. and McComb, A. J.: Plant Resins-Their Formation, Secretion and Possible Functions, Advances in Botanical Research, 6, 277–316, doi:10.1016/S0065-2296(08)60332-8, 1979.

Dentener, F., Stevenson, D., Ellingsen, K., Van Noije, T., Schultz, M., Amann, M., Atherton, C., Bell, N., Bergmann, D., Bey, I., Bouwman, L., Butler, T., Cofala, J., Collins, B., Drevet, J., Doherty, R., Eickhout, B., Eskes, H., Fiore, A., Gauss, M., Hauglustaine, D., Horowitz, L., Isaksen, I. S. A., Josse, B., Lawrence, M., Krol, M., Lamarque, J. F., Montanaro, V., Müller, J. F., Peuch, V. H., Pitari, G., Pyle, J., Rast, S., Rodriguez, J., Sanderson, M., Savage, N. H., Shindell, D., Strahan, S., Szopa, S., Sudo, K., Van Dingenen, R., Wild, O., and Zeng, G.: The global atmospheric environment for the next generation, Environ. Sci. Technol., 40, 3586–3594, doi:10.1021/es0523845, 2006.

Eltayeb, A. E., Kawano, N., Badawi, G. H., Kaminaka, H., Sanekata, T., Shibahara, T., Inanaga, S., and Tanaka, K.: Overexpression of monodehydroascorbate reductase in transgenic tobacco confers enhanced tolerance to ozone, salt and polyethylene glycol stresses, Planta, 225, 1255–1264, doi:10.1007/s00425-006-0417-7, 2007.

Enzell, C. R., Wahlberg, I., and Ryhage, R.: Mass spectra of tobacco isoprenoids, Mass Spectrom. Rev., 3, 395–438, doi:10.1002/mas.1280030304, 1984.

Estell, R. E., Fredrickson, E. L., Anderson, D. M., Mueller, W. F., and Remmenga, M. D.: Relationship of Tarbush Leaf Surface Secondary Chemistry to Livestock Herbivory, Journal of Range Management, 47, 424–428, doi:10.2307/4002991, 1994a.

Estell, R. E., Havstad, K. M., Fredrickson, E. L., and Gardea-Torresdey, J. L.: Secondary chemistry of the leaf surface of Flourensia cernua, Biochemical Systematics and Ecology, 22, 73–77, doi:10.1016/0305-1978(94)90116-3, 1994b.

Fahn, A.: Secretory tissues in vascular plants, New Phytol., 108, 229–257, doi:10.1111/j.1469-8137.1988.tb04159.x, 1988.

Fares, S., Weber, R., Park, J.-H., Gentner, D., Karlik, J., and Goldstein, A. H.: Ozone deposition to an orange orchard: partitioning between stomatal and non-stomatal sinks, Environ. Pollut., 169, 258–266, doi:10.1016/j.envpol.2012.01.030, 2012.

Felzer, B., Reilly, J., Melillo, J., Kicklighter, D., Sarofim, M., Wang, C., Prinn, R., and Zhuang, Q.: Future effects of ozone on carbon sequestration and climate change policy using a global biogeochemical model, Climatic Change, 73, 345–373, doi:10.1007/s10584-005-6776-4, 2005.

Fruekilde, P., Hjorth, J., Jensen, N., Kotzias, D., and Larsen, B.: Ozonolysis at vegetation surfaces, Atmos. Environ., 32, 1893–1902, doi:10.1016/S1352-2310(97)00485-8, 1998.

Goldstein, A. H. and Galbally, I. E

Fu, Y. and Tai, a. P. K.: Known and unexplored organic constituents in the Earth's atmosphereImpact of climate and land cover changes on tropospheric ozone air quality and public health in East Asia between 1980 and 2010, Environ.Sci.Technol., 41, 1514–1521Atmospheric Chemistry and Physics, 15, 10 093–10 106, doi:10.5194/acp-15-10093-2015, 2015.

Gilbert, M. D., Elfving, D. C., and Lisk, D. J.: Protection of plants against ozone injury using the antiozonant N-(1,3-dimethylbutyl)-N'-phenyl-p-phenylenediamine, Bulletin of Environmental Contamination and Toxicology, 18, 783–786, doi:, 2007. 10.1007/BF01691993, 1977.

Goldstein, A. H., McKay, M., Kurpius, M. R., Schade, G. W., Lee, A., Holzinger, R., and Rasmussen, R. A.: Forest thinning experiment confirms ozone deposition to forest canopy is dominated by reaction with biogenic VOCs, Geophys. Res. Lett., 31, L22106, doi:10.1029/2004GL021259, 2004.

Goldstein, A. H. and Galbally, I. E.: Known and Unexplored Organic Constituents in the Earth's Atmosphere, Environmental Science & Technology, 41, 1514–1521, doi:10.1021/es072476p, 2007.

Granier, C., Bessagnet, B., Bond, T., D'Angiola, A., van der Gon, H. D., Frost, G. J., Heil, A., Kaiser, J. W., Kinne, S., Klimont, Z., Kloster, S., Lamarque, J. F., Liousse, C., Masui, T., Meleux, F., Mieville, A., Ohara, T., Raut, J. C., Riahi, K., Schultz, M. G., Smith, S. J., Thompson, A., van Aardenne, J., van der Werf, G. R., and van Vuuren, D. P.: Evolution of anthropogenic and biomass burning emissions of air pollutants at global and regional scales during the 1980-2010 period, Climatic Change, 109, 163–190, doi:10.1007/s10584-011-0154-1, 2011.

Graus, M., Müller, M., and Hansel, A.: High resolution PTR-TOF: quantification and formula confirmation of VOC in real time, J. Am. Soc. Mass Spectr., 21, 1037–1044, doi:10.1016/j.jasms.2010.02.006, 2010.

Hansel, A., Singer, W., Wisthaler, A., Schwarzmann, M., and Lindinger, W.: Energy dependencies of the proton transfer reactions, Int. J. Mass Spectrom., 167–168, 697–703, doi:10.1016/S0168-1176(97)00128-6, 1997.

Heggestad, H. E.: Origin of Bel-W3, Bel-C and Bel-B tobacco varieties and their use as indicators of ozone, Environmental Pollution, 74, 264–291, doi:10.1016/0269-7491(91)90076-9, 1991.

Hewitt, C. N., Kok, G. L., and Fall, R.: Hydroperoxides in plants exposed to ozone mediate air pollution damage to alkene emitters, Nature, 344, 56–58, doi:10.1038/344056a0, 1990.

Himanen, S. J., Blande, J. D., Klemola, T., Pulkkinen, J., Heijari, J., and Holopainen, J. K.: Birch (Betula spp.) leaves adsorb and re-release volatiles specific to neighbouring plants - a mechanism for associational herbivore resistance?, New Phytologist, 186, 722–732, doi:10.1111/j.1469-8137.2010.03220.x, 2010.

Holzinger, R., Lee, A., Paw, K. T., and Goldstein, U. A. H.: Observations of oxidation products above a forest imply biogenic emissions of very reactive compounds, Atmos. Chem. Phys., 5, 67–75, doi:10.5194/acp-5-67-2005, 2005.

IPCC: Climate Change 2013: The Physical Science Basis. Contribution of Working Group I to the Fifth Assessment Report of the Intergovernmental Panel on Climate Change, Cambridge University Press, Cambridge, United Kingdom and New York, NY, USA, 2013.

Isidorov, V. A., Vinogorova, V. T., and Rafałowski, K.: HS-SPME analysis of volatile organic compounds of coniferous needle litter, Atmospheric Environment, 37, 4645–4650, doi:10.1016/j.atmosenv.2003.07.005, 2003.

Jenkin, M. E. and Clemitshaw, K. C.: Ozone and other secondary photochemical pollutants: chemical processes governing their formation in the planetary boundary layer, Atmos. Environ., 34, 2499–2527, doi:10.1016/S1352-2310(99)00478-1, 2000.

Karl, T., Harley, P., Emmons, L., Thornton, B., Guenther, A., Basu, C., Turnipseed, A. and Jardine, K.: Efficient atmospheric cleansing of oxidized organic trace gases by vegetation, Science, 330, 816–819, doi:10.1126/science.1192534, 2010.

Karl, T., Hansel, A., Cappellin, L., Kaser, L., Herdlinger-Blatt, I., and Jud, W.: Selective measurements of isoprene and 2-methyl-3-buten-2-ol based on NO^+ ionization mass spectrometry, Atmos. Chem. Phys., 12, 11877–11884, doi:10.5194/acp-12-11877-2012, 2012.

Kennedy, B. S., Nielsen, M. T., Severson, R. F., Sisson, V. A., Stephenson, M. K., and Jackson, D. M.: Leaf surface chemicals from *Nicotiana* affecting germination of *Peronospora tabacina* (adam) sporangia, J. Chem. Ecol., 18, 1467–1479, doi:10.1007/BF00993221, 1992.

Kennedy, B. S., Nielsen, M. T., and Severson, R. F.: Biorationals from *Nicotiana* protect cucumbers against *Colletotrichum lagenarium* (Pass.) ell. & halst disease development, J. Chem. Ecol., 21, 221–231, doi:10.1007/BF02036653, 1995.

Kurpius, M. R. and Goldstein, A. H.: Gas-phase chemistry dominates O_3 loss to a forest, implying a source of aerosols and hydroxyl radicals to the atmosphere, Geophys. Res. Lett., 30, 1371, doi:10.1029/2002GL016785, 2003.

Laisk, A., Kull, O., and Moldau, H.: Ozone concentration in leaf intercellular air spaces is close to zero, Plant Physiol., 90, 1163–1167, 1989.

Landolt, W., Bühlmann, U., Bleuler, P., and Bucher, J. B.: Ozone exposure–response relationships for biomass and root/shoot ratio of beech (*Fagus sylvatica*), ash (*Fraxinus excelsior*), Norway spruce (*Picea abies*) and Scots pine (*Pinus sylvestris*), Environ. Pollut., 109, 473–478, doi:10.1016/S0269-7491(00)00050-6, 2000.

Langenheim, J. H.: Higher plant terpenoids: A phytocentric overview of their ecological roles, Journal of Chemical Ecology, 20, 1223–1280, doi:10.1007/BF02059809, 1994.

Langenheim, J. H.: Plant Resins: Chemistry, Evolution, Ecology, and Ethnobotany, Timber Press, Portland, Cambridge, 2003.

Lin, Y. and Wagner, G. J.: Surface disposition and stability of pest-interactive, trichome-exuded diterpenes and sucrose esters of tobacco, J. Chem. Ecol., 20, 1907–1921, doi:10.1007/BF02066232, 1994.

Logan, J. a., Staehelin, J., Megretskaia, I. A., Cammas, J. P., Thouret, V., Claude, H., De Backer, H., Steinbacher, M., Scheel, H. E., Stbi, R., Frhlich, M., and Derwent, R.: Changes in ozone over Europe: Analysis of ozone measurements from sondes, regular aircraft (MOZAIC) and alpine surface sites, Journal of Geophysical Research: Atmospheres, 117, 1–23, doi:10.1029/2011JD016952, 2012.

Loreto, F., Mannozzi, M., Maris, C., Nascetti, P., Ferranti, F., and Pasqualini, S.: Ozone quenching properties of isoprene and its antioxidant role in leaves., Plant Physiology, 126, 993–1000, doi:10.1104/pp.126.3.993, 2001.

Loreto, F. and Fares, S.: Is ozone flux inside leaves only a damage indicator? Clues from volatile isoprenoid studies, Plant Physiol., 143, 1096-1100, doi:10.1104/pp.106.091892, 2007.

Massman, W. J.: Toward an ozone standard to protect vegetation based on effective dose: a review of deposition resistances and a possible metric, Atmos. Environ., 38, 2323–2337, doi:10.1016/j.atmosenv.2003.09.079, 2004.

Moldau, H. and Bichele, I.: Plasmalemma protection by the apoplast as assessed from above-zero ozone concentrations in leaf intercellular air spaces, Planta, 214, 484–487, doi:10.1007/s00425-001-0678-0, 2002.

Monson, R. and Baldocchi, D.: Terrestial Biosphere-Atmosphere Fluxes, Cambridge University Press, New York, 2014.

Müller, M., Mikoviny, T., Jud, W., D'Anna, B., and Wisthaler, A.: A new software tool for the analysis of high resolution PTR-TOF mass spectra, Chemometr. Intell. Lab., 127, 158–165, doi:10.1016/j.chemolab.2013.06.011, 2013.

Neubert, A., Kley, D., Wildt, J., Segschneider, H., and Förstel, H.: Uptake of NO, NO_2 and O_3 by sunflower (*Helianthus annuus* L.) and tobacco plants (*Nicotiana tabacum* L.): dependence on stomatal conductivity, Atmos. Environ. A-Gen., 27, 2137–2145, doi:10.1016/0960-1686(93)90043-X, 1993.

Niinemets, Ü., Fares, S., Harley, P., and Jardine, K. J: Bidirectional exchange of biogenic volatiles with vegetation: Emission sources, reactions, breakdown and deposition, Plant Cell Environ., 37, 1790–1809, doi:10.1111/pce.12322, 2014.

Oltmans, S., Lefohn, A., Shadwick, D., Harris, J., Scheel, H., Galbally, I., Tarasick, D., Johnson, B., Brunke, E.-G., Claude, H., Zeng, G., Nichol, S., Schmidlin, F., Davies, J., Cuevas, E., Redondas, A., Naoe, H., Nakano, T., and Kawasato, T.: Recent tropospheric ozone changes – A pattern dominated by slow or no growth, Atmospheric Environment, 67, 331–351, doi:10.1016/j.atmosenv.2012.10.057, 2013.

Ormeño, E., Céspedes, B., Sánchez, I. A., Velasco-García, A., Moreno, J. M., Fernandez, C., and Baldy, V.: The relationship between terpenes and flammability of leaf litter, Forest Ecology and Management, 257, 471–482, doi:10.1016/j.foreco.2008.09.019, 2009.

Palmer-Young, E. C., Veit, D., Gershenzon, J., and Schuman, M. C.: The Sesquiterpenes (E)-ß-Farnesene and (E) - α - Bergamotene Quench Ozone but Fail to Protect the Wild Tobacco Nicotiana attenuata from Ozone , UVB , and Drought Stresses, Plos One, pp. 1–22, doi:10.5061/dryad.602d6, 2015.

Parrish, D. D., Law, K. S., Staehelin, J., Derwent, R., Cooper, O. R., Tanimoto, H., Volz-Thomas, a., Gilge, S., Scheel, H. E., Steinbacher, M., and Chan, E.: Long-term changes in lower tropospheric baseline ozone concentrations at northern mid-latitudes, Atmospheric Chemistry and Physics, 12, 11 485–11 504, doi:10.5194/acp-12-11485-2012, 2012.

Rogge, W. F., Hildemann, L. M., Mazurek, M. A., Cass, G. R., and Simoneit, B. R. T.: Sources of fine organic aerosol. 4. Particulate abrasion products from leaf surfaces of urban plants, Environ. Sci. Technol., 27, 2700–2711, doi:10.1021/es00049a008, 1993.

Sallaud, C., Giacalone, C., Töpfer, R., Goepfert, S., Bakaher, N., Rösti, S., and Tissier, A.: Characterization of two genes for the biosynthesis of the labdane diterpene Z-abienol in tobacco (*Nicotiana tabacum*) glandular trichomes, Plant J., 72, 1–17, doi:10.1111/j.1365-313X.2012.05068.x, 2012.

Schmid, C., Steinbrecher, R., and Ziegler, H.: Partition coefficients of plant cuticles for monoterpenes, Trees, 6, 32–36, doi:10.1007/BF00224496, 1992.

Schnitzler, J. P., Langebartels, C., Heller, W., Liu, J., Lippert, M., Dohring, T., Bahnweg, G., and Sandermann, H.: Ameliorating effect of UV-B radiation on the response of Norway spruce and Scots pine to ambient ozone concentrations, Glob. Change Biol., 5, 83–94, doi:10.1046/j.1365-2486.1998.00208.x, 1999.

Schraudner, M., Moeder, W., Wiese, C., Van Camp, W., Inzé, D., Langebartels, C., and Sandermann, H.: Ozone-induced oxidative burst in the ozone biomonitor plant, tobacco Bel W3, Plant Journal, 16, 235–245, doi:10.1046/j.1365-313X.1998.00294.x, 1998.

Shi, S. and Zhao, B.: Estimating indoor semi-volatile organic compounds (SVOCs) associated with settled dust by an integrated kinetic model accounting for aerosol dynamics, Atmospheric Environment, 107, 52–61, doi:10.1016/j.atmosenv.2015.01.076, 2015.

Singh, S. and Agrawal, S. B.: Impact of tropospheric ozone on wheat (Triticum aestivum L.) in the eastern Gangetic plains of India as assessed by ethylenediurea (EDU) application during different developmental stages, Agriculture, Ecosystems and Environment, 138, 214–221, doi:10.1016/j.agee.2010.04.020, 2010.

Sitch, S., Cox, P. M., Collins, W. J., and Huntingford, C.: Indirect radiative forcing of climate change through ozone effects on the land-carbon sink, Nature, 448, 791–794, doi:10.1038/nature06059, 2007.

Španěl, P., Ji, Y., and Smith, D.: SIFT studies of the reactions of H_3O^+, NO^+ and O_2^+ with a series of aldehydes and ketones, Int. J. Mass Spectrom., 165–166, 25–37, doi:10.1016/S0168-1176(97)00166-3, 1997.

Thimmappa, R., Geisler, K., Louveau, T., O'Maille, P., and Osbourn, A.: Triterpene biosynthesis in plants, Annu. Rev. Plant Biol., 65, 225–257, doi:10.1146/annurev-arplant-050312-120229, 2014.

Van Dingenen, R., Dentener, F. J., Raes, F., Krol, M. C., Emberson, L., and Cofala, J.: The global impact of ozone on agricultural crop yields under current and future air quality legislation, Atmos. Environ., 43, 604–618, doi:10.1016/j.atmosenv.2008.10.033, 2009.

Vickers, C. E., Gershenzon, J., Lerdau, M. T., and Loreto, F.: A unified mechanism of action for volatile isoprenoids in plant abiotic stress., Nature Chemical Biology, 5, 283–291, doi:10.1038/nchembio.158, 2009a.

Vickers, C. E., Possell, M., Cojocariu, C. I., Velikova, V. B., Laothawornkitkul, J., Ryan, A., Mullineaux, P. M., and Hewitt, C. N.: Isoprene synthesis protects transgenic tobacco plants from oxidative stress., Plant, Cell and Environment, 32, 520–31, doi:10.1111/j.1365-3040.2009.01946.x, 2009b.

Vingarzan, R.: A review of surface ozone background levels and trends, Atmos. Environ., 38, 3431–3442, doi:10.1016/j.atmosenv.2004.03.030, 2004.

Wagner, G. J.: Secreting glandular trichomes: more than just hairs, Plant Physiol., 96, 675–679, 1991.

Wagner, G. J., Wang, E. and Shepherd, R. W.: New Approaches for Studying and Exploiting an Old Protuberance, the Plant Trichome, Annals of Botany, 93, 3–11, doi:10.1093/aob/mch011, 2004.

Wang, X. and Mauzerall, D. L.: Characterizing distributions of surface ozone and its impact on grain production in China, Japan and South Korea: 1990 and 2020, Atmos. Environ., 38, 4383–4402, doi:10.1016/j.atmosenv.2004.03.067, 2004.

Weiss, P.: Vegetation/Soil Distribution of Semivolatile Organic Compounds in Relation to Their Physicochemical Properties, Environmental Science & Technology, 34, 1707–1714, doi:10.1021/es990576s, 2000.

Weschler, C. J., Wisthaler, A., Cowlin, S., Tamás, G., Strø m Tejsen, P., Hodgson, A. T., Destaillats, H., Herrington, J., Zhang, J., and Nazaroff, W. W.: Ozone-initiated chemistry in an occupied simulated aircraft cabin, Environmental Science and Technology, 41, 6177–6184, doi:10.1021/es0708520, 2007.

Wisthaler, A., Tamás, G., Wyon, D. P., Strøm Tejsen, P., Space, D., Beauchamp, J., Hansel, A., Märk, T. D., and Weschler, C. J.: Products of ozone-initiated chemistry in a simulated aircraft environment, Environmental Science and Technology, 39, 4823–4832, doi:10.1021/es047992j, 2005.

Wisthaler, A. and Weschler, C. J.: Reactions of ozone with human skin lipids: sources of carbonyls, dicarbonyls, and hydroxycarbonyls in indoor air, P. Natl. Acad. Sci. USA, 107, 6568–6575, doi:10.1073/pnas.0904498106, 2010.

Wohlfahrt, G., Hörtnagl, L., Hammerle, A., Graus, M., and Hansel, A.: Measuring eddy covariance fluxes of ozone with a slow-response analyser, Atmospheric Environment, 43, 4570–4576, doi:10.1016/j.atmosenv.2009.06.031, 2009.

Wohlgemuth, H., Mittelstrass, K., Kschieschan, S., Bender, J., Weigel, H.-J., Overmyer, K., Kangasjarvi, J., Sandermann, H., and Langebartels, C.: Activation of an oxidative burst is a general feature of sensitive plants exposed to the air pollutant ozone, Plant Cell Environ., 25, 717–726, doi:10.1046/j.1365-3040.2002.00859.x, 2002.

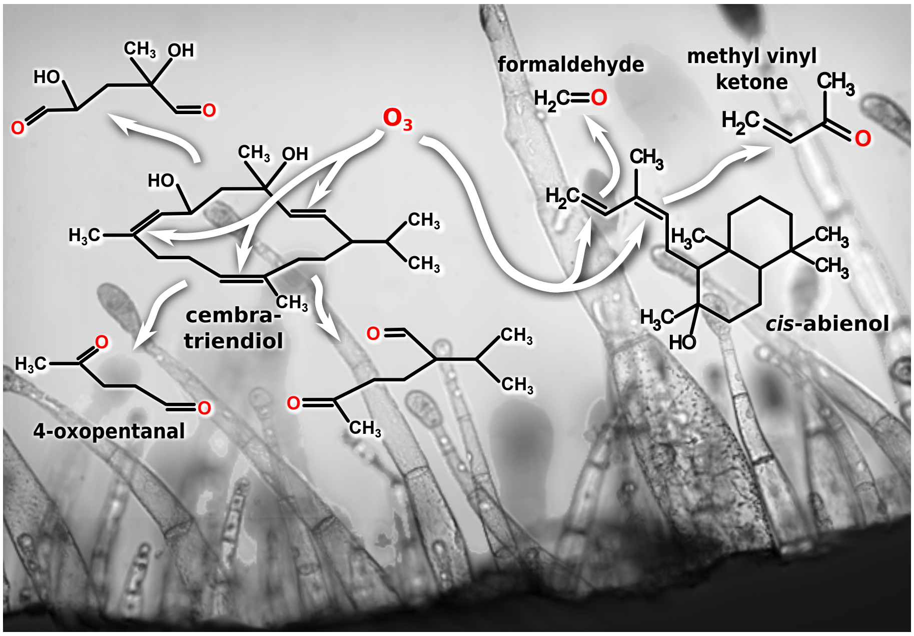

Figure 1. Ozonolysis of diterpenoids exuded by the trichomes of the investigated tobacco plants. The *BYBA* variety releases α- and β-cembratriendiols -cembratrien-diols ($C_{20}H_{34}O_2$), the *Ambalema* variety *cis*-abienol ($C_{20}H_{34}O$); the *Basma Drama* variety exudes all these compounds. Ozonolysis of the cembratriendiols requires at least two ozonolysis steps to form short-chained, volatile carbonyls, like e.g. 4-oxopentanal ($C_5H_8O_2$). Ozonolysis of *cis*-abienol leads to the formation of volatile formaldehyde (HCHO) and methyl vinyl ketone (C_4H_6O).

The background image shows glandular trichomes on a tobacco leaf.

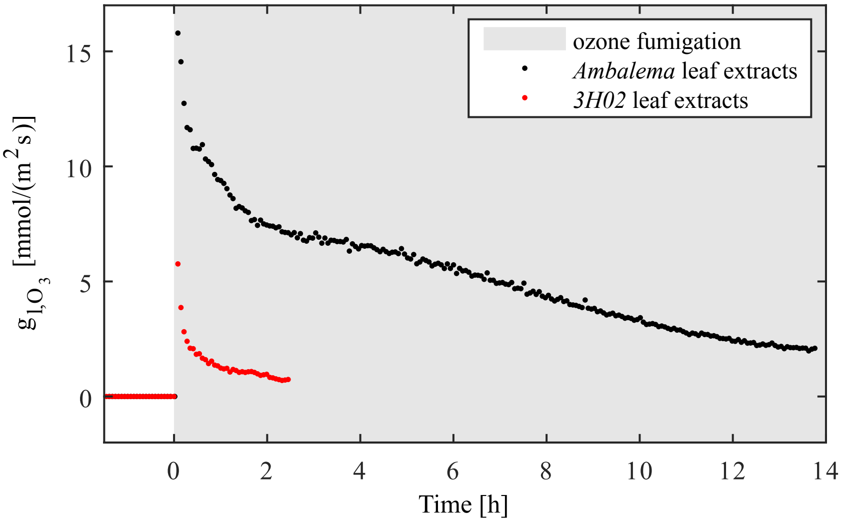

Figure 2. Ozonolysis experiments with pure leaf exudates extracted from non ozone fumigated, unimpaired plants. The leaf extracts containing the surface compounds were applied to the inner surface of the empty plant enclosure system (see Materials and methods section). During ozone fumigation (grey shaded area), the total ozone conductance g_{l,O_3} to the enclosure surface was much higher for *Ambalema* leaf extracts (containing large amounts of the diterpenoid *cis*-abienol) than for 3H02 extracts. Moreover, it remained high for many hours.

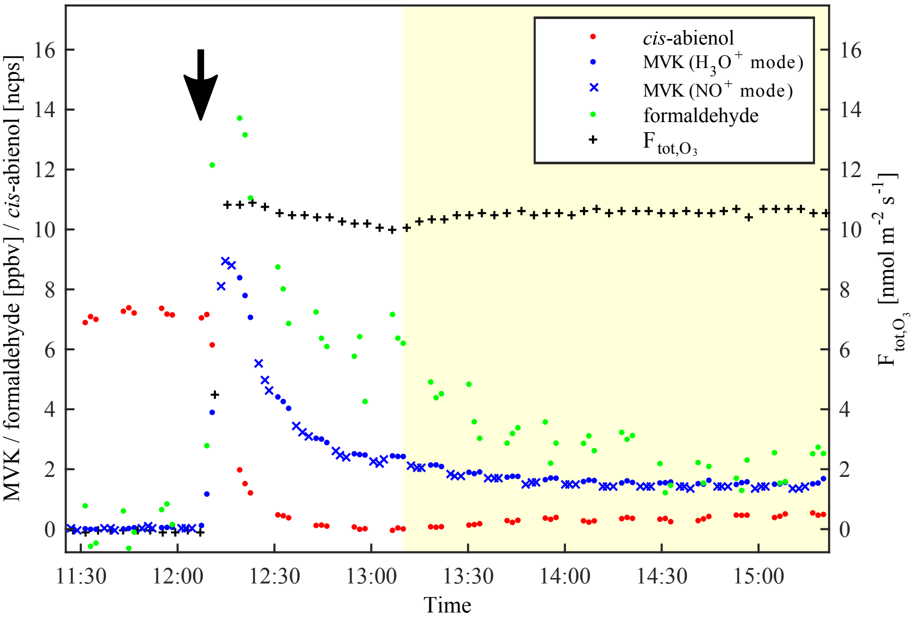

Figure 3. Temporal evolution of selected VOC in an ozonolysis experiment with an *Ambalema* plant and corresponding total ozone deposition flux $F_{\mathrm{tot,O_3}}$. The yellow shaded area denotes time ranges, in which the sample plant was illuminated. Starting the fumigation with ~ 60 ppbv ozone (indicated by the black arrow) the *cis*-abienol signal decreases decreased quickly. At the same time, the carbonyl products of *cis*-abienol ozonolysis, formaldehyde and MVK (measured in $\mathrm{H_3O^+}$ respectively $\mathrm{NO^+}$ reagent ion mode of the SRI-ToF-MS), start started to rise. The large scattering of the formaldehyde signal derives from the strongly reduced sensitivity of the SRI-ToF-MS under high humidity conditions towards this compound. Two hours after the start of the ozone fumigation an equilibrium between actual diterpenoid production and loss due to surface reactions is was established, resulting in stable signals of the oxygenated VOC.

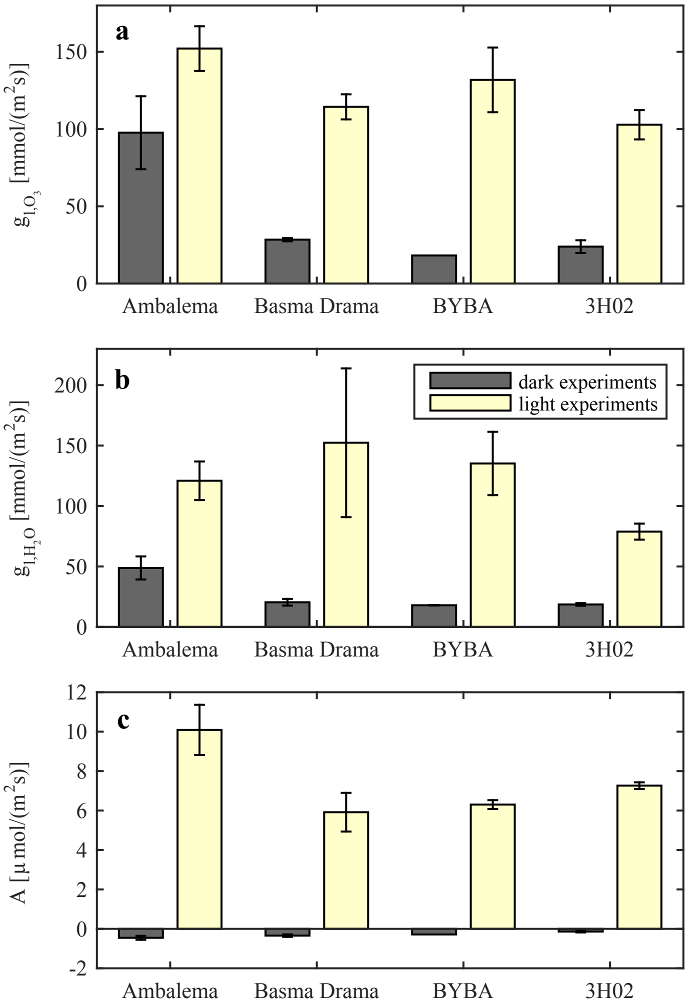

Figure 4. Ozonolysis experiments with pure leaf exudates extracted from non ozone fumigated, unimpaired plants. The leaf extracts containing the surface compounds were applied to the inner surface of the empty plant enclosure system (see Materials and methods section). During Total ozone fumigation conductance g_{l,O_3} (grey shaded area**a**), the total ozone conductance g_{l,O_3} to the enclosure surface was much higher for *Ambalema* leaf extracts than for 3H02extracts. Moreover, it remained high for many hours.Total ozone water vapour conductance g_{l,O_3} g_{l,H_2O} (**b**) and assimilation rates A (**c**) of different tobacco varieties during dark and light conditions. Error bars denote the standard error of 5 (13), 2 (6), 1 (5) and 3 (5) replicates of *Ambalema*, *Basma Drama*, *BYBA* respectively 3H02 in dark (light) experiments. Under dark conditions stomatal ozone conductance is generally low and consequently surface reactions are the major ozone sink. The surface sink is high for the *Ambalema* tobacco line, which exudes *cis*-abienol and lower for the other lines, exuding less reactive or no diterpenoids.

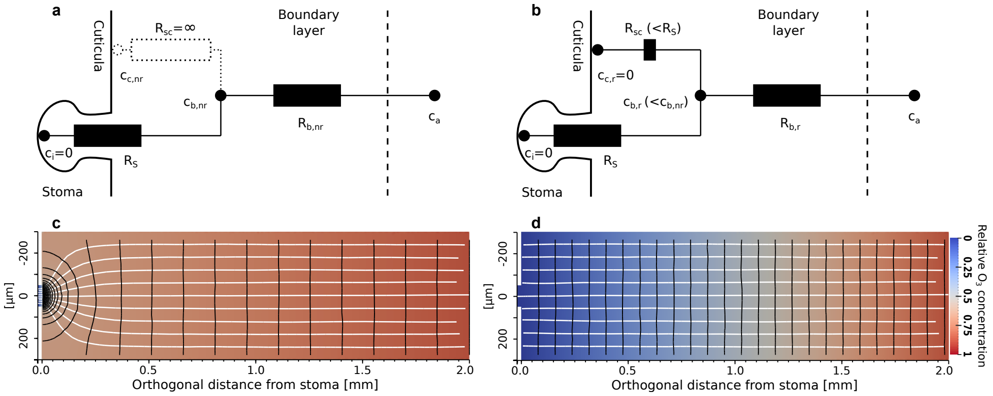

Figure 5. Fluid dynamic calculations of ozone uptake by stomata and leave surface. (**a** and **b**) show the resistance schemes for ozone uptake of leaves with non-reactive (nr) and reactive (r) surfaces. c_i, c_c, c_b and c_a denote ozone concentrations in the stomatal cavity, at the leaf surface, in the boundary layer and in ambient air, respectively. R_s and R_b denote the stomatal and boundary layer resistances. The surface chemical resistance R_sc is infinite ($R_\mathrm{sc} = \infty$) on a non-reactive surface. Fluid dynamic calculations reveal ozone concentration gradients (white lines indicate their orientation) evolving parallel and perpendicular to the leaf surface around the stoma (located at the coordinate (0,0)) in this case (**c**). If the leaf surface is covered with ozone-reactive substances, the parallel fraction of the ozone gradients vanishes, resulting in isosurfaces of ozone concentration (black lines) parallel to the leaf surface and stronger ozone depletion in the leaf boundary layer (**d**).

Marked-up version Supplement

1 The fate of the Criegee BiradicalsIntermediates

In our experiments we focused mainly on stable and volatile ozonolysis products, since these are the only ones directly accessible with SRI-ToF-MS. However, according to current understanding, there are many more possible ozonolysis products. Some of them are very short-lived, others too little volatile and therefore not measurable in the gas phase.

The Criegee mechanism (Criegee, 1975) predicts for gas phase ozone - alkene reactions a decomposition of the primary ozone-alkene addition product into a primary carbonyl compound and a highly excited Criegee Intermediate (CI). On the one hand, unimolecular reactions of unsubstituted (or monosubstituted) anti-CI conformers (terminal oxygen atom faces a hydrogen atom) are believed to yield excited organic acids, which might further dissociate to OH, H and organic radicals (Kroll et al., 2001). On the other hand, unimolecular reactions of disubstituted (or monosubstituted) syn-carbonyl oxides (terminal oxygen faces an alkyl group) are thought to form vinyl hydroperoxide intermediates (Kroll et al., 2001; Cremer, 1981), which will eventually decay forming OH radicals, too. In any case, the OH radicals formed in homogeneous ozone - alkene reactions play an important role in atmospheric chemistry, since their reaction rates with VOC are generally much higher than those of ozone (Atkinson and Arey, 2003). Atmospheric oxidation of VOC in regions with high NO_x concentrations leads again to the formation of ozone (Jenkin and Clemitshaw, 2000). The OH radical recycling is therefore crucial for the oxidizing capacity of the atmosphere.

However, in surface ozonolysis it can be assumed that the energy rich CI is efficiently relaxed through collisions at the surface, thus forming a Stabilized Criegee Intermediate (SCI). If this is the case, we would expect no formation of OH formation from CI in the gas phase. In order to prove this hypothesis we've added cyclohexane as OH scavenger in some of our tobacco experiments. The results indeed indicate that no OH is released into or formed in the gas phase. Nonetheless, we cannot totally exclude OH formation from ozonolysis at the plant surface, where these radicals would be readily scavenged by reactive compounds (e.g. diterpenoids).

In the condensed phase additional reaction pathways for the SCI become available. First, it could undergo a 1,3-cycloaddition with the corresponding ozonolysis carbonyl in order to form a secondary ozonide (Criegee, 1975; Finlayson-Pitts and Pitts, 2000).

Secondly, different isomerisation reactions of the CI could result in stable products. The so-called hot organic acid from anti-CI might be collisionally stabilized at the surface. In the *cis*-abienol case one would expect formic acid from the CI formed in the ozonolysis of the terminal double bond. Formic acid is volatile enough and was detected by SRI-ToF-MS.

In the condensed phase the syn-CI could form a vinyl hydroperoxide which might isomerise to stable α-hydroxy ketones (Epstein and Donahue, 2008). Such molecules were found in ozonolysis experiments of skin oils containing squalene as major constituent (Wisthaler and Weschler, 2010). Indeed, we were able to detect a compound at m/z87.045 ($C_4H_7O_2^+$) and m/z116.035 ($C_4H_6O_2{\bullet}NO^+$) in H_3O^+ respectively NO^+ reagent ion mode, tentatively assigned to α-hydroxy-2-butenone. This compound could be formed along with MVK when the inner double bond of *cis*-abienol (see Fig. 1a) is attacked by ozone.

In the humid plant chamber environment (relative humidity ranged from about 55 % 55 % during dark conditions to $>$ 80 % $>$ 80 % when plants were illuminated) reactions of the SCI in the liquid water layer at the plant surface could also form hydroxy-alkyl hydroperoxides. These could again decay forming carbonyls, acids, hydrogen peroxides, water and OH radicals, as known from gas phase reactions (Hasson et al., 2003).

2 Non-volatile ozonolysis carbonyls

As mentioned in the previous section, fragmentation of the ozone-alkene addition complex yields a carbonyl and a CI. In the case of *cis*-abienol ozonolysis, along with the volatile carbonyls MVK and formaldehyde also the corresponding longer chained carbonyls should be formed. These C_{16} respectively C_{19} compounds are expected to be non-volatile due to their estimated vapour pressure (Goldstein and Galbally, 2007) and will thus remain at the leaf surface. In order to test this, we stripped off the leaf surface compounds after the ozone fumigation experiments as described in the Materials and methods part. The samples were then analysed by GC-MS (see Materials and methods). However, lacking reference spectra of most of the expected non-volatile ozonolysis products, peak assignment was difficult. Nonetheless we could assign a peak with high certainty to sclaral, an isomerisation product of the C_{16} carbonyl from *cis*-abienol ozonolysis. Moreover we were able to detect large amounts of unreacted *cis*-abienol and CBTdiols in samples of the corresponding emitter plant.

3 Surface ozonolysis in tubing and at the plant enclosure surface

The diterpenoids released by the tobacco plants are semi- or low volatile. These terms usually refer to compounds having a low vapour pressure and high boiling point at room temperature (Goldstein and Galbally, 2007). Consequently, under standard conditions they remain mainly in the liquid or solid phase. This is for example the case for the diterpenoid *cis*-abienol, which is a solid at room temperature. Nonetheless, to some extent semi-volatile diterpenoids can evaporate into the gas phase and be deposited in places remote from their point of emission. Continuous condensation and evaporation of the semi-volatile compounds leads to an equilibrium between the gas and condensed phase.

In our experiments plants were installed in the plant enclosure the day before the actual measurement, so that they could adapt and recover from any stress experienced in the course of installation. During plant acclimation the plant enclosure was continuously flushed with clean, ozone free air. Since for example the semi-volatile *cis*-abienol (exuded by the *Ambalema* or *Basma Drama* trichomes) slowly evaporated into the gas phase, it covered over time - when ozone was not present - not only the plant surface, but also the inner surface of the plant enclosure and the downstream tubing system. As a consequence, the *cis*-abienol covered surface area was increased. In the presence of ozone, the adsorbed *cis*-abienol at the enclosure and tubing surfaces was quickly depleted. This effect was responsible for bursts of the volatile diterpenoid oxidation products at the beginning of ozone fumigation (cf. Fig. 23). Eventually, a new equilibrium between diterpenoid production by the plant's trichomes and diterpenoid loss due to surface ozonolysis was established, along with a stable, positive carbonyl signal. Freshly deposited *cis*-abienol was then prevailingly covering the plant surface, which is closest to the trichomes.

To further investigate the impact of the surface ozonolysis in the tubing and at the enclosure surface, additional experiments with two plant enclosures in a row were conducted. To this end, the incoming air stream (see Materials and methods section) was split up in two parts. About $\sim 90\,\%$ $\sim 90\,\%$ of the flow was directed into the first plant enclosure containing a sample plant. The residual part ($\sim 10\,\%$$\sim 10\,\%$) was directed through an ozone generator and could thereby be enriched with ozone. The air containing ozone could then be added either to the first plant enclosure or to the second, empty chamber. Fig. S1 shows the resulting MVK signal from *cis*-abienol ozonolysis in an experiment with an *Ambalema* plant. Ozone addition to the empty plant enclosure caused a short and less intense MVK burst deriving from surface ozonolysis of *cis*-abienol deposited during plant acclimation at the surface of the second chamber and tubing. After about 30 *min* 30 min (~ 3 gas exchange times of the chamber) the MVK signal became insignificant indicating that the surface deposited *cis*-abienol was consumed by ozonolysis and very few *cis*-abienol was resupplied by the air flow originating from the enclosure containing the sample plant. This implicates , that gas phase reactions between *cis*-abienol and ozone are not relevant under fast gas exchange rates.

When in a second step the flow of ozonized air was directed to the first enclosure containing the sample plant, again a large burst of MVK from *cis*-abienol ozonolysis on all surfaces was observed. However, in contrast to the previous experiment, after a certain time span the MVK signal approximated a plateau well above the background level.

4 Relative humidity during ozone fumigation experiments

Several studies have reported on a humidity dependent ozone uptake of different plant types (see e.g. Lamaud et al. (2002); Altimir et al. (2004, 2006))(see e.g. Lamaud et al., 2002; Altimir et al., 2004, 2006). Non-stomatal ozone deposition has been shown to increase significantly above a relative humidity (RH) of about 70 % 70 % (Lamaud et al., 2002; Altimir et al., 2006).

In our experiments the Ambalema variety showed a high total ozone conductance under dark conditions, which was about $4-5$ times higher than that of all other varieties. This cannot be explained by the

RH alone. The relative humidities measured at the enclosure outlet were well below 70 % 70 % in all dark experiments, ranging from ∼ 54 % ∼ 62 % ∼ 54 % – ∼ 62 % (see Table S1). We conclude therefore that the RH had only a minor impact on the total ozone conductance of the varieties tested.

5 2-day simulations of ozone protection through surface diterpenoids

In order to test the long term ozone protection efficiency of a leaf surface covered with diterpenoids, we conducted experiments lasting for two days (see Fig. S2). In the course of these experiments the ozone concentration in the plant enclosure was altered from $0 - 60\ ppbv$0-60 ppbv, mimicking diurnal ozone variations in the atmosphere. In experiments using *cis*-abienol emitters, the start of ozone fumigation led to the well-known rise of the corresponding oxidation products formaldehyde and MVK. Under light conditions and $20\ ppbv$ 20 ppbv ozone the *cis*-abienol signal dropped close to the detection limit. However, during the simulated night and without O_3 fumigation the signal recovered again to pre-fumigation levels. The second day of the experiments closely resembled the first day. Again, at certain ozone levels comparable amounts of oxidation products were formed, correlating with similar levels of overall ozone uptake in the plant enclosure. These results are strong indications that the diterpenoid layer at the surface of the emitting tobacco varieties provides long-term long-term protection against ozone, highlighting its relevance.

6 Resistance scheme for ozone depletion on a semi-reactive leaf surfaceMacroscopic model calculations

Similarly to the microscopic fluid dynamic simulations presented in the main text, we performed macroscopic model calculations (see Materials and methods). These show clearly the beneficial effect of ozone surface reactions. In Fig. S3 the ozone concentration isosurfaces are shown, where the ozone concentration is 10 % of the concentration in air entering the simulated box. For both the non-reactive (Fig. S3a) and the reactive plant (Fig. S3b), ozone uptake by the leaves under the given flow conditions results in an ozone depleted layer around the plant. Leaves located at the downwind side of the plant are generally exposed to less intense ozone stress. If the leaf surface is reactive (Fig. S3a), the ozone depleted layer is broader. When in real forest environments surface reactive plants grow close to each other, intrinsically unprotected plants growing in between benefit from the reduced ozone concentration, too. This effect could find application in agriculture similar to the push-pull concepts used against biotic stressors (Cook et al., 2007).

7 Resistance scheme for ozone depletion on a semi-reactive leaf surface or in the case of non-zero intercellular ozone concentrations

In the main text we showed resistance schemes for ozone depletion on illuminated leaves having a non-reactive (Fig. 5a) and a reactive surface (Fig. 5b). In this respect, reactive means that every ozone molecule hitting the surface is being destroyed, resulting in an ozone concentration of zero at the leaf surface. In nature, however, the surface composition of leaves will always lie some point in between these two extremes: reactive semi-volatile compounds can be deposited on intrinsically non-reactive surfaces and not every ozone molecule hitting a semi-reactive (sr) surface will be destroyed. This situation can be depicted in a slightly more complex resistance scheme as shown in Fig. S4a. When the ozone depletion at the leaf surface is not complete, the ozone concentration in the leaf boundary layer is not equally distributed over the entire leaf surface. The ozone concentration is lowest close to the stomata ($c_{b,sr}c_{\mathrm{b,sr}}$) due to the efficient stomatal sink. At a certain horizontal distance from the stomata, the ozone concentration in the leaf boundary layer ($c^*_{b,sr}c^*_{\mathrm{b,sr}}$) is higher if the surface is semi- or non-reactive. $c^*_{b,sr}$ $c^*_{\mathrm{b,sr}}$ is the reference concentration for the surface chemical resistance $R_{sc,sr}R_{\mathrm{sc,sr}}$.

The concentration gradient caused by the differences between $c_{b,sr}$ and $c^*_{b,sr}$ $c_{\mathrm{b,sr}}$ and $c^*_{\mathrm{b,sr}}$ results in a diffusive ozone transport towards the stomatal pores. This fact is accounted for by introducing an additional resistance $R_x R_{\mathrm{x}}$, which limits this surface parallel transport path.

Conversely, in the case of non-zero intercellular ozone concentration (which has been observed e.g. in experiments applying extremely high ozone concentrations ($> 1\ ppmv$, see Moldau and Bichele (2002)), but perfectly ozone scavenging leaf surface, the ozone concentration would be higher close the stomata and lower at a certain horizontal distance from the stomata. This would result in a diffusive ozone transport away from the stomata, thus eventually further limiting stomatal ozone uptake. In this case the same resistance scheme (Fig. S4a) could be used.

Applying now a Y-Δ transform (Kennelly, 1899), known from electrical circuits, we get the resistance scheme shown in Fig S4b. Here, R'_x, R''_x and $R'_{b,sr}$ R'_{x}, R''_{x} and $R'_{\mathrm{b,sr}}$ can be obtained from R_x, $R_{b,sr}$ and $R^*_{b,sr}R_{\mathrm{x}}$, $R_{\mathrm{b,sr}}$ and $R^*_{\mathrm{b,sr}}$.

The stomatal resistance R_s and R'_x R_{s} and R'_{x} as well as the surface chemical resistance $R_{sc,sr}$ and $R''x$ $R_{\mathrm{sc,sr}}$ and R''_{x} could be combined to single resistances $R'_{s,sr}$ $R'_{\mathrm{s,sr}}$ (= $R_s + R'_x$) and $R'_{sc,sr}$ $R_{\mathrm{s}} + R'_{\mathrm{x}}$) and $R'_{\mathrm{sc,sr}}$ (= $R_{sc,sr} + R''_x R_{\mathrm{sc,sr}} + R''_{\mathrm{x}}$), respectively. This implicates that the resistance scheme for a semi-reactive surface could be modelled similarly to that of a reactive leaf surface (see Fig. 5b). One should bear in mind though, that in this case $R'_{s,sr}$ differs from R_s $R'_{\mathrm{s,sr}}$ differs from R_{s} which is usually attained obtained from the stomatal conductance of water. To be precise, R'_x and R''_x R'_{x} and R''_{x} have to be considered whenever there exists a surface parallel ozone gradient in the leaf boundary layer (cf. Fig. 5a), which is the case for semi- and non-reactive leaf surfaces (and stomata not being infinitely close to each other). R_x R_{x} and therefore also R'_x and R''_x R'_x and R''_x depend strongly on the sink strength of the leaf surface towards ozone. Only in the case of reactive leaf surfaces (cf. Fig. 5b+d) the net surface parallel ozone transport is zero and therefore $R'_{s,sr} = R_s$$R'_\mathrm{s,sr} = R_\mathrm{s}$. While the range of R'_x and R''_x R'_x and R''_x values is difficult to estimate, we want to point out here that disregarding $R_{sc,sr}$ $R_\mathrm{sc,sr}$ will lead to an overestimation of stomatal ozone flux, since $c_{b,sr}$ $c_\mathrm{b,sr}$ strongly depends on the leaf surface sink.

8 Macroscopic model calculations

Similarly to the microscopic fluid dynamic simulations, we performed macroscopic model calculations (see Materials and methods).These show clearly the beneficial effect of ozone surface reactions. In Fig.S3 the ozone concentration isosurfaces are shown, where the ozone concentration is 10 % of the concentration in air entering the simulated box.For both the non-reactive (Fig. S3a) and reactive plant (Fig.S3b), ozone uptake by the leaves under the given flow conditions results in an ozone depleted layer around the plant.Leaves located at the downwind side of the plant are generally exposed to less intense ozone stress.If the leaf surface is reactive (Fig. S3a), the ozone depleted layer is broader.When in real forest environments surface reactive plants grow close to each other, intrinsically unprotected plants growing in between benefit from the reduced ozone concentration, too. This effect could find application in agriculture similar to the push-pull concepts used against biotic stressors (Cook et al., 2007).

References

Altimir, N., Tuovinen, J. P., Vesala, T., Kulmala, M., and Hari, P.: Measurements of ozone removal by Scots pine shoots: Calibration of a stomatal uptake model including the non-stomatal component, Atmospheric Environment, 38, 2387–2398, doi:10.1016/j.atmosenv.2003.09.077, 2004.

Altimir, N., Kolari, P., Tuovinen, J.-P., Vesala, T., Bäck, J., Suni, T., Kulmala, M., and Hari, P.: Foliage surface ozone deposition: a role for surface moisture?, Biogeosciences, 3, 209–228, doi:10.5194/bg-3-209-2006, 2006.

Atkinson, R. and Arey, J.: Atmospheric degradation of volatile organic compounds., Chemical Reviews, 103, 4605–4638, doi:10.1021/cr0206420, 2003.

Cook, S. M., Khan, Z. R., and Pickett, J. A.: The use of push-pull strategies in integrated pest management., Annual review of entomology, 52, 375–400, doi:10.1146/annurev.ento.52.110405.091407, 2007.

Cremer, D.: Theoretical determination of molecular structure and conformation. 7. Stereoselectivity of the ozonolysis reaction, Journal of the American Chemical Society, 103, 3619–3626, doi:10.1021/ja00403a001, 1981.

Criegee, R.: Mechanism of Ozonolysis, Angewandte Chemie International Edition, 14, 745–752, 1975.

Epstein, S. A. and Donahue, N. M.: The kinetics of tetramethylethene ozonolysis: decomposition of the primary ozonide and subsequent product formation in the condensed phase., The journal of physical chemistry. A, 112, 13 535–13 541, doi:10.1021/jp807682y, 2008.

Finlayson-Pitts, B. J. and Pitts, J.: Chemistry of the Upper and Lower Atmosphere, Elsevier, San Diego, doi:10.1016/B978-012257060, 2000.

Goldstein, A. H. and Galbally, I. E.: Known and Unexplored Organic Constituents in the Earth's Atmosphere, Environmental Science & Technology, 41, 1514–1521, doi:10.1021/es072476p, 2007.

Hasson, A. S., Chung, M. Y., Kuwata, K. T., Converse, A. D., Krohn, D., and Paulson, S. E.: Reaction of Criegee Intermediates with Water Vapor - An Additional Source of OH Radicals in Alkene Ozonolysis?, The Journal of Physical Chemistry A, 107, 6176–6182, doi:10.1021/jp0346007, 2003.

Jenkin, M. E. and Clemitshaw, K. C.: Ozone and other secondary photochemical pollutants: chemical processes governing their formation in the planetary boundary layer, Atmospheric Environment, 34, 2499–2527, doi:10.1016/S1352-2310(99)00478-1, 2000.

Kennelly, A.: Equivalence of triangles and three-pointed stars in conducting networks, Electrical World and Engineer, 34, 413–414, 1899.

Kroll, J. H., Sahay, S. R., Anderson, J. G., Demerjian, K. L., and Donahue, N. M.: Mechanism of HO x Formation in the Gas-Phase Ozone-Alkene Reaction. 2. Prompt versus Thermal Dissociation of Carbonyl Oxides to Form OH, The Journal of Physical Chemistry A, 105, 4446–4457, doi:10.1021/jp004136v, 2001.

Lamaud, E., Carrara, A., Brunet, Y., Lopez, A., and Druilhet, A.: Ozone fluxes above and within a pine forest canopy in dry and wet conditions, Atmospheric Environment, 36, 77–88, doi:10.1016/S1352-2310(01)00468-X, 2002.

Moldau, H. and Bichele, I.: Plasmalemma protection by the apoplast as assessed from above-zero ozone concentrations in leaf intercellular air spaces, Planta, 214, 484–487, doi:10.1007/s00425-001-0678-0, 2002.

Wisthaler, A. and Weschler, C. J.: Reactions of ozone with human skin lipids: sources of carbonyls, dicarbonyls, and hydroxycarbonyls in indoor air., Proceedings of the National Academy of Sciences of the United States of America, 107, 6568–75, doi:10.1073/pnas.0904498106, 2010.

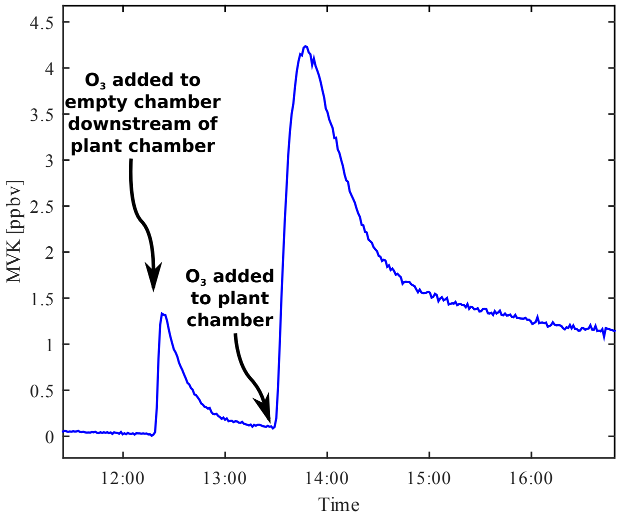

Figure S1: Two chamber ozone fumigation experiment with an *Ambalema* variety. The tobacco plant was installed in a plant enclosure, which was connected to a second, empty chamber at the downstream side. When ozone was added to the empty chamber, the MVK signal deriving from surface ozonolysis of deposited, semi-volatile *cis*-abienol deposited in the empty chamber decreased quickly. When ozone was added to the first plant chamber, the MVK signal approximated a steady state, since the plant surface represented a continuous diterpenoid source. In this steady state, *cis*-abienol ozonolysis occurred prevailingly at the plant surface. For details refer to the text.

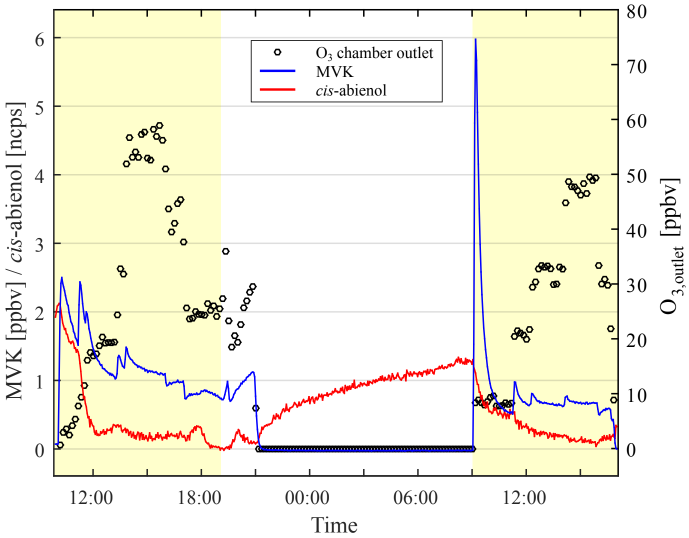

Figure S2: Experiment with an *Ambalema* plant simulating diurnal ozone variations. Yellow shaded areas represent times when the plant was illuminated. Addition of ozone resulted in in an immediate reduction of the signal of semi-volatile *cis*-abienol and an initial MVK burst, deriving from *cis*-abienol ozonolysis on all surfaces. The *cis*-abienol signal recovered over night, leading to a huge MVK burst from surface ozonolysis at 09:00AM after restarting the ozone fumigation.

Resistance scheme of ozone uptake by a plant leaf with a semi-reactive (sr) surface. c_i, c_c, c_b and c_a denote ozone concentrations in the stomatal cavity, at the leaf surface, in the boundary layer and in ambient air, respectively. R_s, R_{sc} and R_b denote the stomatal, surface chemical and boundary layer resistances. R_x limits the surface parallel ozone transport in the leaf boundary layer from the cuticula towards the stomatal pores. The resistance scheme in **a** can be transformed into that shown in **b** by applying a Y-Δ transform. For details refer to the text.

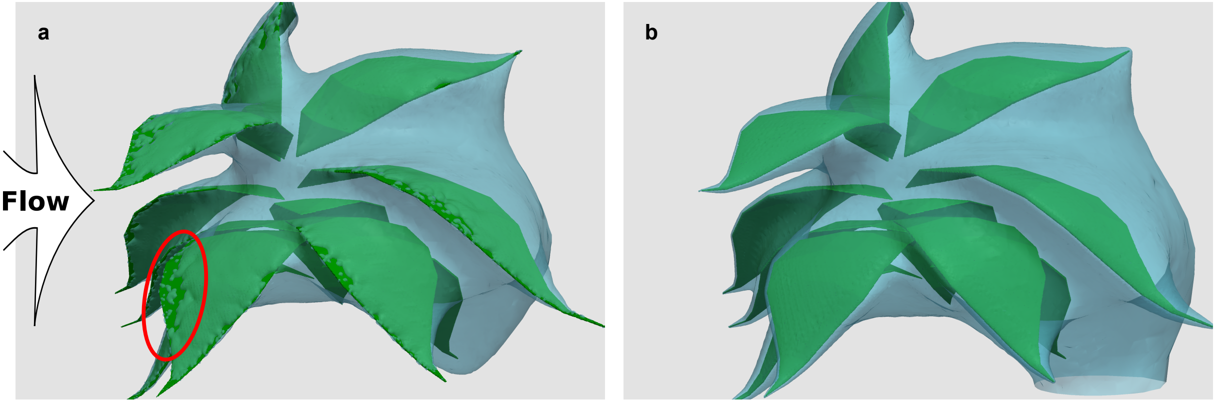

Figure S3: Macroscopic fluid dynamic calculations. The plots show the isosurfaces (in light blue color) of equal ozone concentration obtained from model simulations, in which similar plants without (**a**) or with (**b**) ozone-reactive leaf surface were fumigated with ozonated air (entering from the left side). The concentration at the isosurfaces corresponds to 10 % 10 % of the ozone concentration in the advecting air. In the case of a non-reactive leaf surface (**a**), solely stomatal uptake is responsible for the reduced ozone concentration in the leaf boundary layer. In places directly exposed to the advecting ozone-rich air, the leaf surface itself is exposed to high ozone concentrations (above the 10 % limit, see e.g. the area indicated by the red ellipse). In contrast, ozonolysis at the plant surface further reduces the ozone concentration in the air layer adjacent to the leaf surface (**b**). As a result, the reactive leaf surface expands the ozone depleted area. This effect, in combination with the lack of the pore effect for ozone on reactive leaf surfaces, diminishes the amount of phytotoxic ozone entering the leaf stomata.

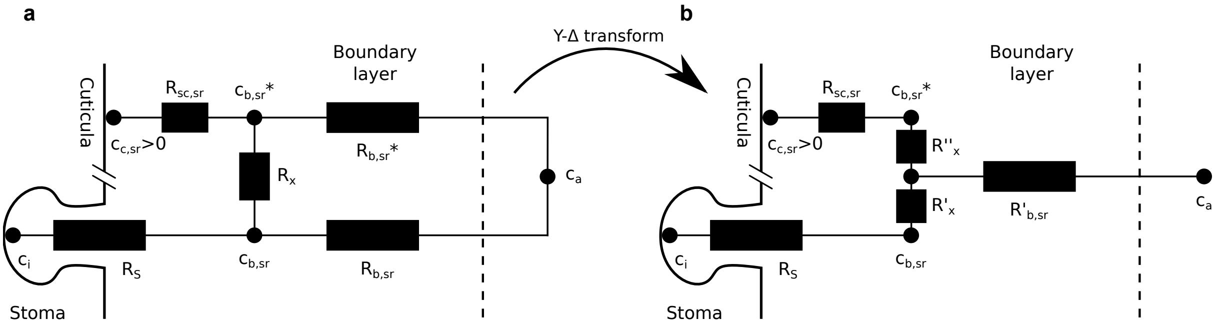

Figure S4: Resistance scheme of ozone uptake by a plant leaf with a semi-reactive (sr) surface or in the case of non-zero intercellular ozone concentrations (c_i). c_c, c_b and c_a denote ozone concentrations at the leaf surface, in the boundary layer and in ambient air, respectively. R_s, R_sc and R_b denote the stomatal, surface chemical and boundary layer resistances. R_x limits the surface parallel ozone transport in the leaf boundary layer from the cuticula towards the stomatal pores. The resistance scheme in **a** can be transformed into that shown in **b** by applying a Y-Δ transform. For details refer to the text.

Table S1: assimilation rates A and relative Relative humidities RH in the plant enclosure during ozone fumigation experiments of different tobacco varieties. Values are given for the same time ranges, for which the total ozone conductance has been calculated (see Fig. 4) and include standard errors of 5 (13), 2 (6), 1 (5) and 3 (5) replicates of *Ambalema*, *Basma Drama*, *BYBA* respectively *3H02* in dark (light) experiments.

	RH [%]	
Plant variety	dark	light dark light
Ambalema	0.45 ± 0.10 -10.09 ± 1.27 62 ± 2	78 ± 2
Basma Drama	0.34 ± 0.06 -5.92 ± 0.98 55 ± 2	79 ± 4
BYBA	0.29 -6.30 ± 0.23 60	86 ± 1
3H02	0.14 ± 0.04 -7.26 ± 0.17 54 ± 2	76 ± 2

Values are given for the same time ranges, for which the total ozone conductance has been calculated (see Fig. 4) and include standard errors of 5 (13), 2 (6), 1 (5) and 3 (5) replicates of *Ambalema*, *Basma Drama*, *BYBA* respectively *3H02* in dark (light) experiments. The sign of the assimilation rate is reported from an atmospheric point of view with a negative sign corresponding to a net uptake by the plants.